The Impact of Galaxy Mergers on Planes of Satellite Galaxies

– Dissertation –

MPhys Physics with Astronomy

Kosuke Kanehisa

November 2021

Student ID: 6406042

Supervisor: Dr. Marcel Pawlowski

University of Surrey
Faculty of Engineering and Physical Sciences
Department of Physics
Guildford GU2 7XH
United Kingdom

Declaration:

Abstract

Highly flattened and co-rotating planes of dwarf satellite galaxies have been observed around the Milky Way, M31, and Centaurus A in the Local Volume. The imprinting of angular momentum from host galaxy mergers has been raised as a potential formation mechanism for satellite planes. I investigate the effects of major mergers on M31 and Centaurus A-like dark matter haloes for the first time in a full cosmological context, using the IllustrisTNG hydrodynamic cosmological simulations. Recent mergers with mass ratios of 1:3 or above generally have a negligible impact on the phase-space correlation of the most massive satellites at present time. The post-merger accretion of new satellites is responsible for washing out the effects of mergers. Furthermore, satellites that participated in a merger are stripped of mass and removed from the sample of the most massive satellites. This process reduces the merger's influence on the full present-day satellite distribution to a minimal degree after $2-5$ Gyr. When solely considering satellites that participated in the full duration of a merger, mergers appear to prevent the formation of highly flattened satellite systems with minor-to-major axis ratios of $c/a < 0.3$. The radial extents of satellite distributions are reduced post-merger due to tidal disruption and subsequent infall, resulting in lower plane heights but near-constant axis ratios. Major mergers are unlikely to form correlated planes of (primordial) satellite galaxies in a full cosmological context.

Acknowledgments

Foremost, I would like to express my deepest gratitude to my supervisor, Dr. Marcel Pawlowski, for giving me the opportunity to pursue my dream career in astrophysics. Your encouragement and guidance over the past year has been invaluable, and your unwavering support throughout the difficulties of studying abroad and the exceptional work environment during the pandemic has made all the difference.

I would also like to thank the experts who were extremely helpful in my Master's placement: Dr. Oliver Müller, for his insightful advice and help regarding various aspects of this research, and Dr. Michelle Collins, for her support throughout my time at Surrey and abroad.

To my good friend Will: thank you for always being there, and for bearing with me on long tangents about my research. Our long calls and game nights gave me a sense of normality in this tough year.

Finally, I must express my unending gratitude to my parents, who have supported and encouraged me every step of the way. Thank you for always believing in me and pushing me forward – this achievement wouldn't have been possible without you.

Contents

List of Figures

List of Tables

List of Abbreviations

CASP	Centaurus A Satellite Plane
CDF	Cumulative Distribution Function
DMO	Dark Matter Only
GPoA	Great Plane of Andromeda
KS	Kolmogorov-Smirnov
ΛCDM	Lambda Cold Dark Matter
M31	The Andromeda Galaxy
MPB	Main Progenitor Branch
RMS	Root Mean Square
TDG	Tidal Dwarf Galaxy
ToI	Tensor of Inertia
VPOS	Vast Polar Structure

1 Introduction

In 1920, astronomers Harlow Shapely and Heber Curtis came head-to-head at the Smithsonian Institution in a public series of lectures now known as the Great Debate. Their purpose was to discuss the true nature of *spiral nebulae* and the size of the Milky Way, which was then believed to span the entirety of the observable universe. Shapely argued that observed *nebulae* were not local to the Milky Way, but independent galaxies much like our own. Later that decade, Shapely's views were vindicated by Edwin Hubble. Hubble used the stable periodicity of Cepheid variable stars to measure the distance to the M31 *nebula* to be around 300 kpc (Hubble). This was an order of magnitude larger than the then-estimated extent of the Milky Way (Shapley).

Just over a century later, we now know that the Local Group, a spherical region of space spanning a diameter of 3 Mpc in which we reside, contains more than 80 galaxies (Nadler et al.). The Local Group is dominated by its two most massive inhabitants, the Milky Way and the Andromeda Galaxy (M31). Most other local galaxies are orbitally bound to either in the form of satellites like a planet orbits its host star. These dwarf satellite galaxies are generally substantially less massive than their highly luminous host galaxies, making their detection difficult. While several – such as the Large and Small Magellanic Clouds around the Milky Way – are visible with the naked eye, most of the Local Group's satellite galaxy population were only first observed within the last decade, owing to the deployment of modern astronomical surveys (*e.g.* Koposov et al.) such as the Sloan Digital Sky Survey (Blanton et al.) and the Dark Energy Survey (Abbott et al.).

The bountiful population of known satellite galaxies far outnumbers the larger host galaxies they are bound to, and form discrete galactic systems (rather than being evenly distributed throughout the cosmos). The Local Volume, a region of space spanning a diameter of 20 Mpc centered on the Local Group, consists of over 500 galaxies (Karachentsev et al.). Most of these galaxies are constrained within the Local Group, the Sculptor Group, and the Centaurus A Group. The Centaurus A Group is populated by a still-growing number of nearly 50 observed satellite galaxies (Crnojević, Grebel, and Koch). It is gravitationally dominated by two major host galaxies, Centaurus A and M83, at respective distances of 3.7 Mpc and 4.6 Mpc from the Milky Way.

1.1 Planes of Satellite Galaxies

In 1976, a curious discovery was made by Kunkel and Demers and Lynden-Bell. The six then-known satellite galaxies of the Milky Way, along with streams of high-velocity gas, were found to align with a plane passing through the Milky Way's galactic centre. This strange structure was hypothesized to be the remnants of another galaxy's merger with the Milky Way.

We now know that most of the luminous satellite galaxies around the Milky Way follow a highly planar distribution called the Vast Polar Structure (VPOS; Pawlowski, Pflamm-Altenburg, and Kroupa). This plane has a root-mean-square (RMS) height as low as 30 kpc (Pawlowski, McGaugh, and Jerjen), and is oriented at a nearly perpendicular angle to the Milky Way's galactic disk. The VPOS is also traced by a population of globular clusters – dense, spherical collections of stars that are substantially less massive than dwarf galaxies – and stellar and gaseous streams (Metz, Kroupa, and Jerjen). Measurements of the satellite galaxies' proper motions, changes in their apparent on-sky positions, further indicate that up to 9 out of 11 members of the VPOS may be orbiting within their defined plane (Pawlowski and Kroupa).

This highly correlated plane of satellite galaxies does not appear to be unique to the Milky Way. Signs were found as early as the late 20th century (Grebel, Kolatt, and Brandner) that a subset of the then-known satellites around M31 followed a similar structure. Precise observations from modern astronomical surveys in the past decade such as the Pan-Andromeda Archaeological Survey (McConnachie et al.) have lead to an unprecedented, detailed view of M31's satellite galaxies. 15 out of 27 satellites form an extremely thin structure named the Great Plane of Andromeda (GPoA), which has a RMS plane height of around 12 kpc (Conn et al.). Similar to the VPOS, up to 13 out of 15 of the GPoA's plane members appear to be co-rotating (Ibata et al.).

Observing satellite systems outside of the Local Group is challenging due to the vast distances involved. Measurement uncertainties from common distance metrics such as the Tip of the Red Giant Branch method exceeds the Milky Way's virial radius at distances of over 5 Mpc, making the resolution of satellite distances difficult (Pawlowski). Nevertheless, a number of studies have investigated satellite galaxy distributions around Local Volume host galaxies outside of the Local Group.

The most popular candidate is Centaurus A, an elliptical galaxy at a distance of 3.8 Mpc from the Milky Way. It features an irregular morphology that may have

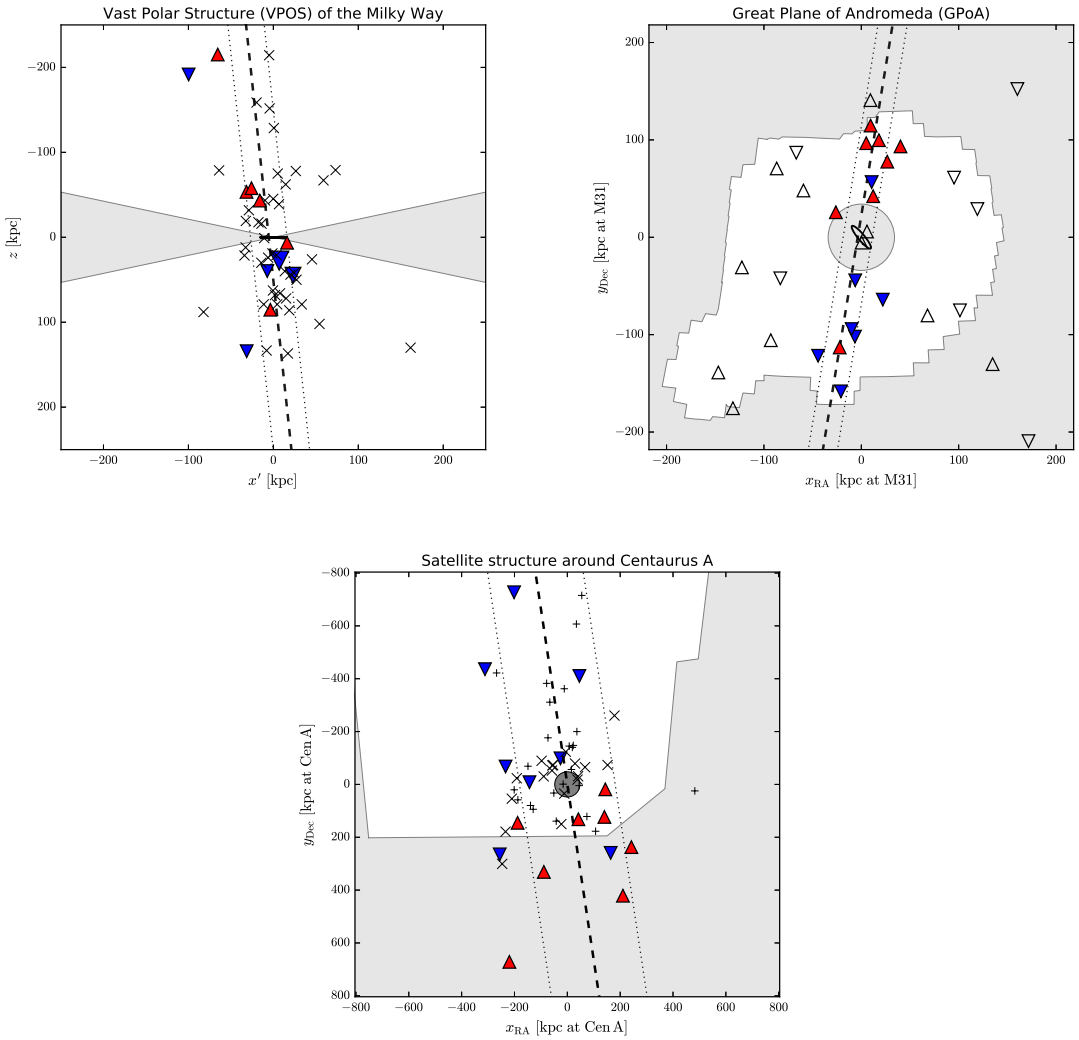

Figure 1: Adapted from Pawlowski. *Upper Left Panel:* The VPOS as seen from a position where both the satellite plane and the Milky Way's galactic disk (black line) is edge-on. *Upper Right Panel:* The on-sky GPoA as seen from the Milky Way. *Bottom Panel:* The on-sky CASP as seen from the Milky Way. In all panels, the relevant satellite plane is drawn in dashed black lines, while white (gray-shaded) areas represent observable (unobserved) areas in the relevant astronomical survey. Satellite galaxies with known velocities are drawn in triangles – red and blue triangles indicate receding and approaching satellites with respect to the recession velocity of the host galaxy.

arisen from a recent galaxy merger (Wang et al.). Centaurus A's estimated mass (Tully) is greater than that of the Milky Way (Taylor et al.) and M31 (Tamm et al.), making the system easier to observe despite its distance. Intriguingly, Centaurus A also appears to host a plane of satellite galaxies – albeit thicker than the VPOS

or GPoA, with a RMS plane height of around 140 kpc (Müller et al.). Up to 21 out of 28 members of the Centaurus A Satellite Plane (CASP) are reported to be co-rotating (Müller et al.). See Figure 1 for a diagram of the Milky Way, M31, and Centaurus A's satellite distributions.

The presence of flattened, co-rotating planes of satellite galaxies around the three largest Local Volume host galaxies presents an interesting riddle for modern theories of galaxy formation. This is referred to as the Planes of Satellite Galaxies Problem (Pawlowski).

There are indications that such correlated structures may be ubiquitous in the wider cosmos. M81 and M101, which are spiral galaxies even further from the Milky Way than Centaurus A, were also reported to host thin planes of dwarf galaxies (Chiboucas et al.; Müller et al.). Furthermore, an abundance of diametrically opposed satellite galaxy pairs with anti-correlated velocities were found in the Sloan Digital Sky Survey, which may trace co-rotating structures (Ibata et al.).

The extent to which galaxies outside of the Local Volume host satellite planes is still uncertain. However, this may change with the completion of upcoming projects such as the SAGA survey (Geha et al.), which aims to detect satellite galaxies at distances of more than 20 Mpc.

1.2 Satellites in a Cold Dark Matter Cosmology

The Lambda Cold Dark Matter model (ΛCDM) is the current concordance model – the most widely accepted and frequently used model of cosmology. The ΛCDM model posits that the universe consists of three distinct components. Visible baryonic matter, consisting of protons, neutrons and everything composed of them, only accounts for $\approx 5\%$ of the Universe's mass-energy budget. The remaining 95% consists of invisible, non-relativistic dark matter (27%) and dark energy, responsible for the late acceleration of Hubble expansion (68%) (Planck Collaboration). This cosmological model has been greatly successful at matching cosmological phenomena at large scales, including the prediction of current stellar helium abundances from a process known as primordial nucleosynthesis, microscopic fluctuations in the Cosmic Microwave Background (Planck Collaboration), and the large-scale structure of the Universe (Eckert et al.).

In the ΛCDM paradigm, baryonic structures such as visible galaxies are hosted in massive clumps of dark matter called haloes. They span distances many times the

diameter of the central baryonic component. Dark matter haloes are gravitationally bound structures decoupled from the expansion of the Universe, and form the basic unit of cosmological structure.

As haloes gradually decrease in density from their central regions outwards and cannot be directly observed, it is difficult to precisely characterize their size or mass using traditional techniques. We instead describe their size and mass by their *virial radius* and *virial mass* respectively. The virial radius represents the radius of the halo at which the enclosed dark matter is sufficiently overdense to detatch from the expansion of the Universe and form a bound structure. Here, we use an overdensity of $200\rho_{crit}$ as per convention, where ρ_{crit} is the critical density of the Universe. The virial mass represents the mass contained within the virial radius of a given halo.

Haloes grow via hierarchical clustering, wherein small dark matter haloes merge to form larger haloes over cosmic time (Davis et al.). This process corresponds to the merging and growth of the hosted baryonic components, forming the galaxies and other cosmological structures observable today. When smaller haloes fall into larger host haloes, they may survive the accretion process as bound objects in the form of subhaloes within the host halo (Moore et al.). Such dark matter substructures form a population of satellites within the host halo (Metz and Kroupa), while their baryonic components are observable as satellite galaxies orbiting around a more massive host galaxy.

The distribution of subhaloes around a host is predicted to be somewhat isotropic (randomly distributed) in a ΛCDM universe, a natural consequence of the chaotic merger process during the haloes' hierarchical growth (Kroupa, Theis, and Boily). It is debated whether this underlying dark matter substructure is fully traced by the observable, luminous satellite galaxy population (Zentner et al.; Libeskind et al.; Libeskind et al.).

1.3 Cosmological Simulations

The development of cosmological simulations has greatly contributed in advancing our understanding of structural formation in the Universe over the last decades. These simulations model various astrophysical processes over a set of initial conditions, producing "toy universes" that span cosmological volumes. High-resolution ΛCDM simulations specifically, which model the evolution of cold dark matter haloes in a dark energy-dominated environment, have been successful in generating simulated universes very similar to our own (*e.g.* Fattahi et al.; Springel et al.). These

simulated universes, which are individual realisations of a ΛCDM cosmology, may be considered theoretical predictions of the underlying model. These predictions may be tested by comparing them with the results of astronomical surveys at various scales.

Kroupa, Theis, and Boily first noted that the degree of spatial and kinematic correlation observed in the Milky Way's brightest satellites appeared to be in conflict with the near-isotropic distribution of subhaloes expected in a ΛCDM model of structure formation. Assuming that luminous satellite galaxies evenly traced an underlying isotropic distribution of dark matter substructure, they argued, the VPOS was incompatible with such a distribution by a confidence of 99.5%. Zentner et al. and Libeskind et al. disagreed with Kroupa, Theis, and Boily's assumption, separately demonstrating that a certain degree of substructure anisotropy is common in dark matter-only N-body simulations (Kravtsov, Klypin, and Khokhlov; Springel, Yoshida, and White). Luminous satellites are only formed in the largest subhaloes before their accretion into the host galaxy's halo, and those largest subhaloes are not necessarily isotropically distributed. Additionally, the local structure of the Cosmic Web defines preferential directions of satellite accretion, which further intensifies the resultant anisotropy. Such anisotropic distributions were also observed in the local Universe by Brainerd and Yang et al. using the Sloan Digital Sky Survey. For a time, it appeared that the conflict had been resolved.

However, the degree of natural anisotropy from the effects above is insufficient to match the highly correlated, co-rotating planes of satellites in the Local Volume. Only $5 - 10\%$ of Milky Way-like haloes hosted satellite distributions as flattened as the VPOS (Wang, Frenk, and Cooper) in the Millennium-II dark matter-only simulations (Boylan-Kolchin et al.). When considering the angular momentum unit vectors of the observed satellites, which are known as orbital poles, only 0.44% of simulated satellite systems matched the orbital correlation of the VPOS (Pawlowski et al.).

Similarly, GPoA-like satellite distributions, defined by simultaneously constraining radial extent, plane thickness, and number of co-orbiting satellites, were only hosted by less than 0.2% of M31-like haloes in Millennium-II (Ibata et al.; Pawlowski et al.). Analogs of the Centaurus A system are also rare. Systems matching the on-sky flattening and co-orbiting population of the then-known 16 satellites with distance and velocity measurements only occurred at a frequency of 0.1% in Millennium-II (Müller et al.). Searching for Centaurus A analogs in the hydrodynamic Illustris simulation (Vogelsberger et al.), which incorporates baryonic components such as

gas and stars along with the underlying dark matter structure, yielded a similarly rare frequency of 0.5%.

This discrepancy between the degree of satellite anisotropy between Local Volume systems and analogs in cosmological simulations presents a serious small-scale challenge against the ΛCDM model of structure formation, which has otherwise been highly successful at matching the structure and evolution of the Universe at large scales. Astronomers have suggested several potential solutions for these satellite planes, the most prominent of which are briefly covered in Section 1.4.

1.4 Suggested Solutions

After Kroupa, Theis, and Boily first pointed out the anisotropy of the Milky Way's most luminous satellite galaxies, Zentner et al. and Libeskind et al. demonstrated that subhaloes are accreted from preferential directions defined by a system's orientation to local Cosmic Web filaments. Lovell et al. additionally discovered that this *filamentary accretion* process generated flattened, co-rotating systems of satellites within Milky Way-like haloes in the Aquarius dark matter-only simulations (Springel et al.). However, a follow-up study by Pawlowski et al. found that VPOS-like satellite distributions were still rare at 0.44%.

Furthermore, filaments local to the Milky Way and M31 have effective diameters that are wider than their haloes' virial radii (Vera-Ciro et al.; Ibata et al.), and cannot reproduce the small RMS heights of the VPOS and GPoA. While the natural anisotropy of ΛCDM subhalo distributions due to filaments indicates that the use of an isotropic null-hypothesis to determine the significance of a plane (*e.g.* Kroupa, Theis, and Boily) is flawed, filamentary accretion cannot individually account for the strong correlation observed in Local Group satellites.

Considering the similar orbits of satellites within the VPOS, GPoA and CASP, it is natural to expect some shared history. One hypothesis suggests that a large group of gravitationally bound dwarf galaxies may have fallen into a host halo in a single accretion event, resulting in correlated angular momenta and orbital trajectories. Li and Helmi were one of the first to investigate this *group infall* hypothesis, determining that the emergence of the VPOS was inevitable if all the Milky Way's satellites fell in as a single group. However, they found that only up to a third of the VPOS members could have realistically fallen in as a group – *i.e.* the thin observed plane is not reproducible.

Additionally, such dwarf galaxy groups are too spatially extended to produce the thin plane heights of observed Local Volume satellite systems (Metz et al.). Large group infall events are also rare – most satellites were found to be accreted individually in Milky Way analogs in the Aquarius simulations (Wang, Frenk, and Cooper). A similar trend was reported for M31-like systems in Millennium-II (Shao et al.). The most extreme events only brought in up to a half of the VPOS population. As angular momenta and orbits are only shared among the accreted group, group infall is unlikely to be the sole cause of satellite planes in the Local Vroup.

While the filamentary accretion and group infall hypotheses assume that the observed satellite galaxies are dark matter-dominated substructures, they may also be of tidal origin – implying that satellites are purely baryonic objects with no underlying dark matter subhaloes (Kroupa). Such Tidal Dwarf Galaxies (TDGs) form when two galaxies interact via a fly-by or merger, forming tidal debris consisting of dust and gas that collapses under self-gravity. Further star formation within the dense resultant cloud can produce dwarf galaxies with similar observable properties to dark matter-dominated dwarfs. TDGs may account for a substantial fraction of observed dwarf galaxy populations (Okazaki and Taniguchi), can have lifespans of more than several Gyr (Ploeckinger et al.), and have been detected in cosmological simulations (Ploeckinger et al.; Haslbauer et al.).

As TDGs form from a common tidal event, they may conceivably share similar angular momenta and orbital trajectories. The degree of orbital correlation observed in the VPOS was found to be reproducible from a tidal origin in simulations (Pawlowski et al.), and both co-orbiting and counter-orbiting material emerges as a natural consequence of galaxy interactions (Pawlowski, Kroupa, and De Boer). Similarly, a hypothetical ancient merger of M31 was reported to be compatible with the current positions and velocities of GPoA members (Fouquet et al.; Hammer et al.).

However, the application of TDGs to the Planes of Satellite Galaxies Problem is faced with several criticisms. As TDGs originate from the material of a separate interacting galaxy, their metallicities should be distinct from dark matter-dominated satellites (Kirby et al.). However, on-plane and off-plane satellites around M31 have similar metallicities (Collins et al.). Furthermore, Local Group satellites have high mass-to-light ratios, implying that their masses are dominated by dark matter (Wolf et al.). Finally, if a majority of VPOS and GPoA members were tidal, there would be a dearth of highly luminous, dark matter-dominated substructure compared to that predicted by ΛCDM (Pawlowski, Pflamm-Altenburg, and Kroupa). Circumventing

these issues would require the invocation of non-ΛCDM cosmologies such as Modified Newtonian Dynamics (*e.g.* Milgrom; Bılek et al.), which rejects the existence of dark matter entirely.

At present, there is no consensus on a singular formation mechanism for observed satellite planes. The existing hypotheses cannot fully explain the strong flattening and orbital correlation of Local Volume satellite systems, or else requires a cosmology other than the concordance ΛCDM model.

1.5 Mergers as a Formation Mechanism

An alternative, straightforward consequence of mergers between two host galaxies is the imprinting of the merger's trajectory and angular momentum upon the satellite galaxy populations of both participating hosts. While not extensively studied in literature, it is conceivable that such imprints may induce some co-rotating motion within the post-merger halo.

The histories of two Local Volume hosts, M31 and Centaurus A, makes mergers a potentially interesting line of inquiry. Both may have experienced major mergers within the last several Gyr. M31 is thought to have merged with the smaller M32 galaxy's progenitor around 2 Gyr ago, with a merger mass ratio of $\approx$ 1:3 (D'Souza and Bell; Hammer et al.). Similarly, Centaurus A's disturbed morphology may have arisen from a violent merger 2 Gyr ago with a mass ratio of $\approx$ 1:1.5 (Wang et al.). If mergers between host galaxies tend to strengthen the kinematic correlation and flattening of their satellite galaxy distributions, the tension between M31 and Centaurus A's satellite planes and their respective analogs in ΛCDM cosmological simulations could be weakened or resolved.

A seminal study by Smith et al. explored the consequences of mergers on satellite distributions in an isolated environment. They considered merger events between two dark matter haloes with initial mass ratios of up to 1:1. In Smith et al., the smaller, *secondary* host halo contained 10 satellites, while the larger, *primary* host halo was devoid of substructure. They varied the mass ratio between merging host haloes, the initial distribution of satellites within the secondary halo, and the trajectory in which the secondary halo enters the merger.

Smith et al. found that three main factors were responsible for determining whether a merger would generate an anisotropic satellite plane. Firstly, the distribution of satellites along the axis perpendicular to the plane in which the merger occurs,

the *merger plane*'s normal vector $\hat{h}$, was found to be strongly representative of the height of the final halo's satellite distribution. Satellites were slung outwards along the merger plane due to the merger's angular momentum, while their displacement along $\hat{h}$ was less affected. If the initial satellite distribution along $\hat{h}$ was small, the increase in satellites' radial distances from the host after being slung out generated a flattened plane.

Next, the secondary halo needed to enter the merger at a near-circular orbit to generate thin satellite planes. An initially circular orbit corresponds to a large magnitude of angular momentum imprinted upon the two merging satellite distributions, which in turn slung satellites out further along the merger plane.

Finally, a majority of satellites within the secondary halo needed to be *prograde*, or have initial angular momenta roughly aligned with the angular momentum imprinted from the halo's merger. Prograde satellites, initially orbiting the secondary host galaxy in the same direction as the merger's in-spiral motion, were slung out to larger distances. On the other hand, retrograde satellites, with orbits opposing the merger's in-spiral motion, experienced reduced angular momenta – leading to a loss in tangential velocity and a subsequent infall into the merged halo's centre. There, the retrograde satellites were stripped of mass by tidal forces and destroyed. As a result, only initially prograde satellites were found in any resultant satellite plane.

Smith et al. demonstrated that thin planes of satellites, with root-mean-square (RMS) heights as low as 40 kpc, could be formed through mergers when the three factors above were fulfilled. These generated planes were also co-rotating, matching the behaviour of the three Local Volume satellite planes. However, their assumption that only the secondary, smaller halo contained satellites is unrealistic. As the authors themselves point out, the primary halo should contain a larger population of satellites in proportion to its mass ratio with the secondary halo. If the primary halo's mass dominates over the secondary halo's mass, satellites bound to the primary halo would be substantially less affected by the merger's angular momentum.

Two scenarios are possible, depending on the merger's mass ratio. For mass ratios $\ll$ 1:1, only satellites initially bound to the secondary halo should participate in any resultant plane – leading to less than one half of the final halo's satellite population forming a flattened configuration. This is at odds to the richly populated satellite planes observed in the Local Volume.

On the other hand, if the mass ratio is $\approx$ 1:1, satellites from both the primary and secondary haloes may participate. However, to generate a flattened plane of satellites

in this scenario, the distribution of satellites along the merger plane's normal vector $\hat{h}$ for both merging haloes would need to be simultaneously constrained to the resultant plane's height, which is much less likely to occur.

1.6 Study Outline

It is currently unclear whether the three criteria outlined by Smith et al. are commonly fulfilled simultaneously in the local Universe, and whether mergers can explain the curious anisotropy of satellite planes observed around M31 and Centaurus A. In this study, I test for correlation between the spatial and kinematic coherence of satellite galaxy planes and the timing and magnitude of recent major mergers in a full cosmological context. I investigate M31 and Centaurus A-mass haloes within a ΛCDM hydrodynamic cosmological simulation, aiming to determine whether mergers – along with appropriate initial conditions – can generate flattened, co-rotating satellite planes.

This dissertation is organized as follows. In Section 2, I introduce the simulation analysed, my method for sampling simulated systems, the parameters used to quantify phase-space correlation in satellite distributions, and some statistical methods for determining the significance of said parameters. Using these tools, I explore the extent of the anisotropy found in simulated satellite systems.

Section 3 investigates the influence of observationally motivated systems' merger histories on the strength of their phase-space correlation at present time. I additionally consider the kinematics of each system's last major merger, quantifying the impact that merger trajectory and stability has on satellite distributions.

In Section 4, I present evidence that the influence of mergers on present-time satellite distributions is washed out by post-merger satellite accretion and the mass stripping of merger-participating satellites. By defining samples purely consisting of participant satellites, and tracking their phase-space distribution at different stages of their history, I reveal the full impact mergers have on correlation in satellite systems.

Finally, in Section 5, I summarize my findings and discuss some of their implications for explaining planes of satellite galaxies in our own Universe. Some potential future work is also discussed.

2 Systems at Present Time

2.1 The IllustrisTNG Simulation

Cosmological simulations serve as valuable realisations of an underlying cosmological model. Due to their vast simulation volumes, researchers can generate large statistical samples of satellite galaxy systems. Simulated systems also lack the measurement uncertainties inherent in observation methods. Assuming that all relevant astrophysical processes are accurately modelled and realized, cosmological simulations present alternative universes for study that are functionally similar to ours.

In this study, data was drawn from the IllustrisTNG cosmological simulation, specifically the TNG 100-1 run (Springel et al.; Pillepich et al.). IllustrisTNG is a hydrodynamic simulation, which incorporates the effects of baryonic processes such as stellar feedback and supernovae, as well as the hierarchical growth of dark matter haloes in a Planck ΛCDM cosmology (Planck Collaboration).

Most previous comparisons to simulations that disregard the possibility of TDGs (*e.g.* Wang, Frenk, and Cooper; Ibata et al.; Müller et al.) used dark matter-only (DMO) simulations. High-resolution, large-volume hydrodynamic simulations have only been available in recent years, with the release of Illustris (Vogelsberger et al.) in 2014 and the EAGLE hydrodynamic simulation (McAlpine et al.) in 2016. Furthermore, short-range baryonic processes are not expected to play a large role in the formation of satellite galaxy systems – a process concerned with the movement of substructure within a host halo at a scale of hundreds of kpc. DMO simulations also generally boast higher mass resolutions, which aids in identifying smaller substructures.

I elected to use the IllustrisTNG simulation for the following reasons. Firstly, the inclusion of baryonic physics strengthens the tidal forces in the central regions of haloes. This intensifies the tidal disruption of satellites within these central regions, resulting in radial distributions that are less centrally concentrated (Garrison-Kimmel et al.). In turn, this results in a minor difference in the morphology of satellite distributions (*e.g.* Müller et al.). Hydrodynamic simulations should produce the most similar satellite configurations to those in our own Universe.

TNG100 offers a dark matter particle mass of $7.5 \times 10^6 M_\odot$ over a simulation volume of $(110\ \text{Mpc})^3$. This is sufficient to clearly resolve smaller satellite galaxies with $M_{dm} \approx 10^9 M_\odot$, while retaining enough individual systems for a full statistical analysis. The alternative TNG300 run offers a larger sample size over $(300\ \text{Mpc})^3$, but

at the cost of a resolution reduced by an order of magnitude ($M_{dm} = 5.9 \times 10^7 M_\odot$). Here, data was drawn from TNG100 due to its higher resolution, but this study may be repeated using TNG300 for additional insights.

IllustrisTNG uses snapshots to record the evolution and growth of dark matter haloes and subhaloes over time. Snapshots are moments in simulated cosmic time, and are separated by intervals of $\approx 100 - 200$ Myr. Available snapshots are bound by snapshot 99 (present time, corresponding to an age of 13.80 Gyr) and snapshot 0 (an universe with an age of 0.18 Gyr). For each snapshot, all existing haloes and subhaloes are identified by their respective catalogs. To track the same subhalo over time, IllustrisTNG incorporates a comprehensive *Sublink* merger tree (Rodriguez-Gomez et al.). For each snapshot, Sublink records whether a certain subhalo merged with another to form a *descendant* in the following snapshot, as well as the subhalo's *progenitor* in the previous snapshot. These features aid in identifying the merger history of simulated systems at present time.

2.2 Sampling Systems

Haloes were sampled from the TNG100-1 halo catalog at present time. Sampling was done in two *mass regimes*, roughly analogous to the masses of Centaurus A and M31's haloes. The masses of Centaurus A and M31 were referenced to find realistic, yet sufficiently different mass regimes found within the Local Universe. The selection of the two host galaxies was motivated by their violent merger history. Our sampled systems will not be directly compared to the GPoA and CASP in this study.

I define a *large-bin*, Centaurus A-like halo to have a virial mass of $M_{vir} = (4.0 - 12.0) \times 10^{12} M_\odot$. The large-bin sample was constrained to isolated haloes by rejecting large-bin haloes with companion haloes above $0.25 M_{vir}$ within 800 kpc. These criteria are motivated by the estimated virial mass of Centaurus A at $M_{200} = 8.0 \times 10^{12} M_\odot$ (Tully) and mirrors that used in Müller et al. to identify Centaurus A analogs.

Similarly, I define a *small-bin*, M31-like halo to have a virial mass of $M_{vir} = (1.0 - 2.0) \times 10^{12} M_\odot$. An isolation criteria was imposed by rejecting small-bin haloes with companion haloes above $0.25 M_{vir}$ within 500 kpc. These criteria are motivated by the estimated virial mass of M31 at $(0.8 - 1.1) \times 10^{12} M_\odot$ (Tamm et al.).

Next, the most prominent satellites bound to each *host* halo at present time were identified. There are two methods by which this can be done. We may simply select a radial distance (usually the halo's virial radius) from the centre-of-mass of the halo, and define all subhaloes within the resultant sphere as satellites. This is analogous to observing a galactic system within our Universe, though other factors such as survey biases, satellite kinematics and spectroscopy would also be considered. This approach is common in studies that compare observed satellite distributions to simulated analogs (*e.g.* Müller et al.; Pawlowski et al.), due to its similarity to observational methods. However, this approach also risks misidentifying unrelated structures that are temporarily close to the the host halo, as well as rejecting bound satellites outside the defined radius.

As the aim of this study is to determine the manner in which recent mergers affect satellite distributions in a general capacity, it is to our benefit to obtain a comprehensive catalog of satellites, even if several outliers may have not been recognized as satellites if the systems were physically observed. Thus, it is wiser to identify subhaloes that are bound to host haloes as satellites, drawing data from IllustrisTNG's halo and subhalo catalogs. A halo's central subhalo, referred to as simply the *central* in later sections, is defined as the largest-mass subhalo bound to the host halo. All other subhaloes bound to the host halo are designated as *satellites*.

For each host halo in both mass regimes, the 30 satellites with the largest dark matter mass M_{dm} were identified. Each selected satellite must also be linked to a corresponding Main Progenitor Branch (MPB) merger tree, demonstrating a history of more than one snapshot. If a system lacked 30 satellites with MPB merger trees, it was excluded from consideration. A total of 298 large-bin, 820 small-bin systems were identified for analysis.

2.3 Methods for Measuring Correlation

For each system sampled in Section 2.2, I calculated the distances, $s_{sat,i}$, and velocities, $v_{sat,i}$, of each of the 30 satellites relative to their corresponding central. I also recorded the magnitudes of the satellites' relative distances and velocities, $|s_{sat,i}|$ and $|v_{sat,i}|$, and assigned them to randomly oriented unit vectors drawn from an isotropic distribution. The resultant set of phase-space coordinates, $s_{rand,i}$ and $v_{rand,i}$, serves as an isotropic distribution of satellites to compare simulated distributions with, while controlling for bias from satellite radial distance profiles. In this study, these isotropic satellite distributions are called *randomized* systems.

2.3.1 Spatial Correlation

For each system, a set of $N_{grid} = 10000$ points were generated isotropically on a unit sphere. Each point represents a unit vector, $\hat{r}_j$. For $j = [1, 10000]$, we may define a plane passing through the central with a normal vector of $\hat{r}_j$. The orthogonal RMS distance $\Delta_{rms,j}$ of all 30 satellites to each plane was calculated as

$$\Delta_{rms,j} = \sqrt{\sum_{i=1}^{30} |s_{sat,i} \cdot \hat{r}_j|^2}. \tag{1}$$

The *best-fit plane* of a satellite system is described by $\hat{r}_j$ for the instance of j when $\Delta_{rms,j}$ reaches its minimum value. Note that a plane's RMS height, $\Delta_{rms,j}$, is not equivalent to the absolute plane height, which considers the distance to satellites on both sides of the best-fit plane.

Based on a system's best-fit plane, the spatial properties of its satellite distribution are described by the following parameters.

1. Δ_{rms}, the RMS plane height.
2. c/a, the minor-to-major axis ratio of the satellite distribution.
3. $N_{coorb,plane}$, the number of satellites co-rotating in one direction about $\hat{r}$.

To determine c/a for a given system, a Tensor-of-Inertia (ToI) fit was separately applied. For a set of satellite positions $s_{sat,i}$, the ToI is calculated as

$$T(s) = \sum_{i=1}^{30} (s_{sat,i}^2 \cdot I) - (s_{sat,i} \cdot {s_{sat,i}}^T) \tag{2}$$

where I is the identity matrix, and $T(s)$ is the ToI of the system (see Pawlowski et al.). $T(s)$ has three eigenvalues, $\lambda_1 \leq \lambda_2 \leq \lambda_3$. The eigenvector x_1 corresponding to λ_1 describes the major axis of the system's satellite distribution. Substituting $\hat{x_1}$ for $\hat{r}_j$ in Equation 1, the RMS spread of satellites over the major axis for each system was calculated as a. The minor-to-major axis ratio was then calculated as $c/a = \Delta_{rms}/a$, representing the scale-free degree of flattening of each system's satellite distribution.

$N_{coorb,plane}$ was determined using the following procedure. For each system, the direction of each satellite's angular momentum was calculated as

$$\hat{l}_i = \frac{s_{sat,i} \times v_{sat,i}}{|s_{sat,i} \times v_{sat,i}|}. \tag{3}$$

For each satellite, a parameter m_{rot} was found as

$$m_{rot,i} = \hat{l}_i \cdot \hat{r}, \tag{4}$$

where $m_{rot,i}$'s sign indicates whether a satellite is orbiting clockwise or counterclockwise relative to $\hat{r}$. I defined $N_{coorb,plane}$ as the number of satellites with positive or negative $m_{rot,i}$, whichever is greater. Thus, the number of co-orbiting satellites is limited to the range $N_{coorb,plane} = [15, 30]$.

Parameters Δ_{rms}, c/a, and $N_{coorb,plane}$ were determined for all large-bin and small-bin simulated satellite systems, as well as their randomized counterparts. It is important to note that lower c/a and Δ_{rms} values correspond to a stronger degree of spatial flattening and correlation, while higher values of $N_{coorb,plane}$ represent a stronger tendency to co-rotate.

2.3.2 Kinematic Correlation

To express the degree of kinematic correlation in simulated satellite systems, an analysis was performed similarly to Section 2.3.1. A set of $N_{grid} = 10000$ points was generated isotropically on a unit sphere. Each point represents a unit vector, $\hat{p}_j$. For $j = [1, 10000]$, The RMS angle between each satellite's angular momentum unit vector $\hat{l}_i$ and grid unit vector $\hat{p}_j$ was calculated as

$$\angle_{rms,j} = \sqrt{\sum_{i=1}^{30} [cos^{-1}(\hat{l}_i \cdot \hat{p}_j)]^2}. \tag{5}$$

The *best-fit orbital pole* of a satellite system is described by $\hat{p}_j$ for the instance of j when $\angle_{rms,j}$ reaches its minimum value. Based on the best-fit orbital pole, the kinematic properties of a system's satellite distribution are described by the following parameters.

1. $\angle_{rms}$, the RMS angular deviation of satellite orbital poles, or the orbital pole concentration.

3. $N_{coorb,orbit}$, the number of satellites co-rotating in one direction about $\hat{p}$.

$N_{coorb,orbit}$ was defined in a manner similar to $N_{coorb,plane}$, using $\hat{p}$ instead of $\hat{r}$ as the orbital axis. $\angle_{rms}$ and $N_{coorb,orbit}$ were determined for all large-bin and small-bin simulated satellite systems, as well as their randomized counterparts. A lower $\angle_{rms}$ represents a higher degree of kinematic correlation, while higher values of $N_{coorb,orbit}$ – like its counterpart in $N_{coorb,plane}$ – corresponds to a higher degree of co-rotation in a satellite system.

2.3.3 Statistical Significance

When discussing parameters of spatial or kinematic correlation in the following sections, we may express their significance with respect to a specified background distribution. This background distribution may be associated with the randomized, isotropic sample of satellite systems, or else serve as a comparison between systems with different merger histories. Assuming that the given background distribution is Gaussian, the parameter's significance z is calculated as

$$z = \frac{x - \mu}{\sigma} \tag{6}$$

where x is the specific value of the parameter, μ is the mean of the background distribution, and σ is the standard deviation of the background distribution. This method may be less applicable for discrete or highly non-Gaussian parameters such as $N_{coorb,plane}$ or $N_{coorb,orbit}$.

2.3.4 The Pearson Correlation Coefficient

When considering a possible link between two variables, I used the Pearson correlation coefficient, or Pearson's r, as my primary measure of correlation. Pearson's r is a measure of correlation that ranges between -1 and 1 between two variables that are assumed to be normally distributed and linearly correlated. Due to these assumptions, r will not always be an accurate representation of the strength of the relationship between two variables. However, it can still indicate whether two variables are fully uncorrelated ($r \approx 0$), strongly positively correlated ($r \approx 1$) or strongly negatively correlated ($r \approx -1$). For a given sample with two variables, x and y, Pearson's r is calculated as

$$r_{xy} = \frac{\sum_{i=1}^{n}(x_i - \bar{x})(y_i - \bar{y})}{\sqrt{\sum_{i=1}^{n}(x_i - \bar{x})^2}\sqrt{\sum_{i=1}^{n}(y_i - \bar{y})^2}} \tag{7}$$

where n is the number of data points within the sample. $\bar{x}$ and $\bar{y}$ represents the respective means of x and y.

Assuming normality and linearity, a p-value can be calculated for a derived value of r. Given the null-hypothesis that the two variables are not correlated is true, p represents the probability that the observed set of data could be obtained. If a p-value is low ($p < 5\%$), there is insufficient evidence to reject the null-hypothesis.

In this study, calculations of r between correlation parameters and the corresponding p-values were done through the `pearsonr` implementation in the SciPy package (Virtanen et al.).

2.3.5 The Kolmogorov-Smirnov Test

The Kolmogorov-Smirnov (KS) test is a method of comparing one-dimensional probability distributions. Put simply, it measures the degree of similarity between distributions. The one-sample KS test compares an obtained distribution with a background distribution, while the two-sample KS test compares two obtained distributions with each other. Here, the latter is useful when comparing how the distributions of correlation parameters differ between mass regimes, and whether related parameters (*e.g.* $N_{coorb,plane}$ and $N_{coorb,orbit}$) form identical distributions.

Let the empirical cumulative distribution functions (CDFs) of the two distributions be $F(x)$ and $G(x)$, with m and n data points respectively, where x is the common variable. The two-sample KS test measures the maximum deviation between the CDFs (see Figure 2), which is expressed as the two-sample KS statistic D:

$$D = max_x|F(x) - G(x)|. \tag{8}$$

If m and n are sufficiently large, the maximum deviation expected if the two CDFs are drawn from the same distribution – known as the *critical value* – is expressed as

$$D_\alpha = c(\alpha)\sqrt{\frac{m+n}{mn}}. \tag{9}$$

$c(\alpha)$, a function of the chosen significance threshold α, is calculated as

$$c(\alpha) = \sqrt{-\frac{1}{2}ln(\frac{\alpha}{2})}. \tag{10}$$

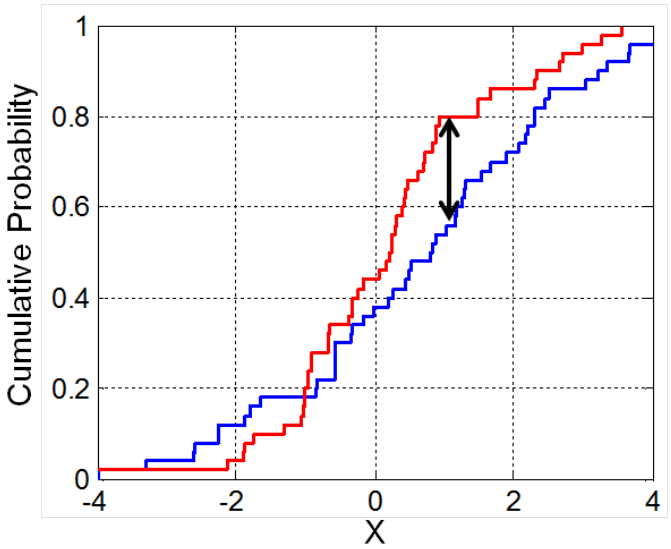

Figure 2: A demonstration of the two-sample KS statistic. The black arrow represents the maximum deviation between the two empirical CDFs (red and blue lines). *Credit: Wikimedia Commons.*

The null-hypothesis for the two-sample KS test is that the two observed distributions are drawn from the same base distribution. If $D > D_\alpha$, with a small corresponding p-value, the null-hypothesis may be rejected – there is sufficient evidence to show that the two distributions are distinguishable.

2.4 Correlation in Sampled Systems

To gain an understanding of the degree of anisotropy expected in the sampled satellite distributions, I initially disregarded any role that recent mergers may play. In this section, I discuss the general distribution of correlation parameters for the entire population of satellite systems sampled in Section 2.2. See Section 3 and later sections for comparisons with individual merger histories.

2.4.1 General Results

The distributions of c/a, Δ_{rms}, and $\angle_{rms}$, three key correlation parameters that describe the spatial and kinematic anisotropy of the sampled satellite systems, are shown in Figure 3. Simulated systems consistently demonstrate a stronger degree of correlation (expressed as lower c/a, Δ_{rms}, or $\angle_{rms}$) in all three parameters.

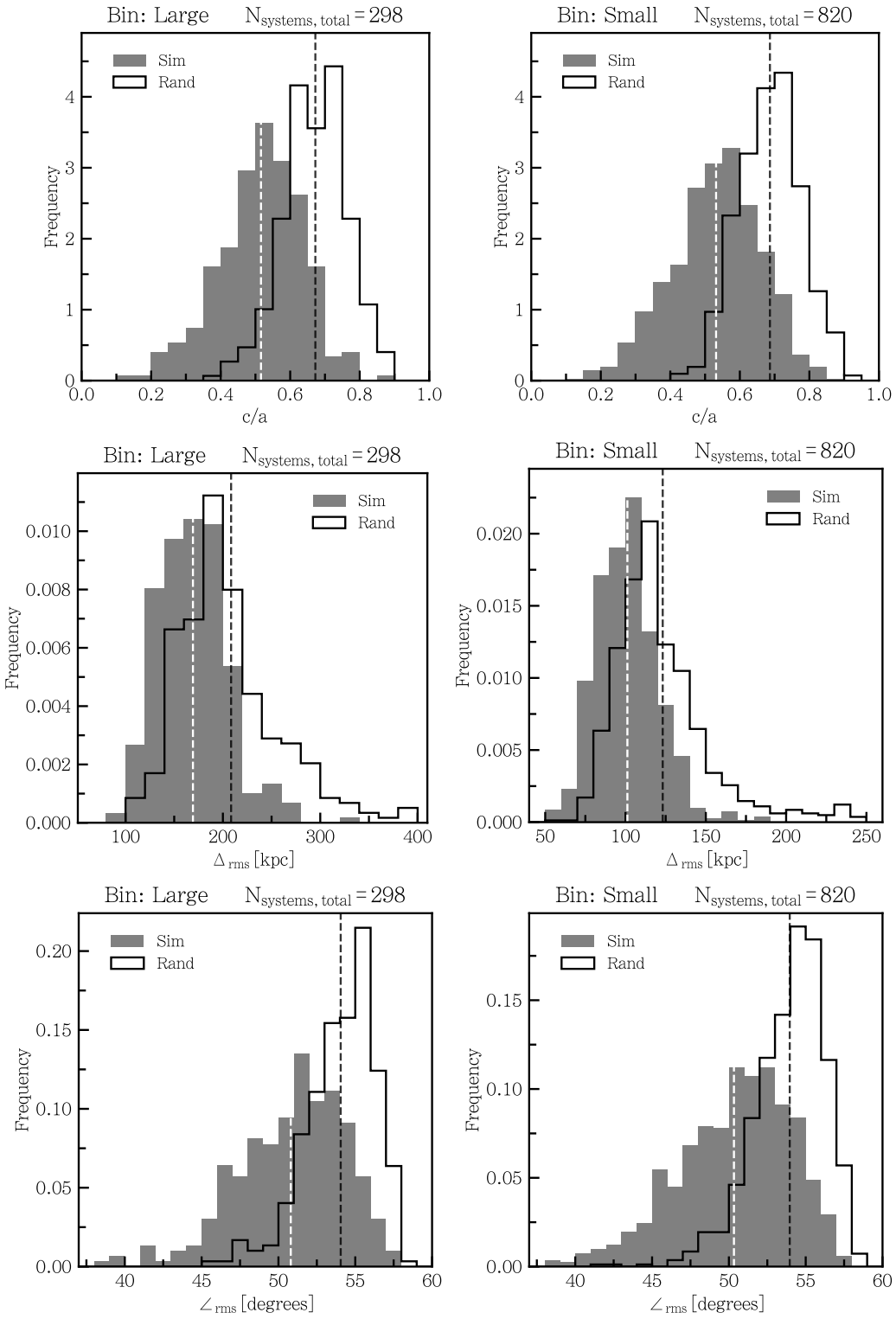

Figure 3: Distributions of c/a, Δ_{rms}, and $\angle_{rms}$ for large-bin and small-bin systems. Simulated systems are drawn in grey, while their randomized counterparts are drawn in black outlines. White and black dashed lines indicate mean values for simulated and randomized systems respectively. Simulated systems consistently demonstrate a stronger degree of correlation with respect to isotropy.

This trend is most visible for c/a. The mean c/a value for simulated large-bin and small-bin systems is shifted towards enhanced flattening with respect to isotropy, at 1.7σ and 1.7σ respectively. Notably, no randomized system in either mass regime reaches $c/a < 0.35$, while the most correlated simulated systems demonstrate $c/a < 0.15$.

The simulated c/a distributions for large-bin and small-bin systems initially appear similar, with $c/a_{large} = 0.52 \pm 0.12$ and $c/a_{small} = 0.53 \pm 0.13$. However, a KS test determined that the two distributions are distinguishable, with only a 4.5% change of being drawn from the same distribution. This data suggests that the flattening of satellite distributions varies slightly by host mass, and is not scale-free.

A similar trend can be seen for Δ_{rms}. While the distance scale of the two mass regimes are different, preventing a direct comparison, the simulated systems consistently demonstrate lower values of Δ_{rms}, which indicates a thinner distribution. With mean values of $\Delta_{rms,large} = 169 \pm 35$ kpc and $\Delta_{rms,small} = 101 \pm 19$ kpc, the simulated systems diverge from from their randomized counterparts by 0.7σ and 0.7σ for large-bin and small-bin systems respectively.

Curiously, the minimum plane heights found for simulated and randomized systems only differ by 5 kpc for large-bin systems and 3 kpc for small-bin systems. This may imply that highly flattened systems, as indicated by low c/a, may be a product of a greater plane extent than a thinner plane. I also point out the "tail" of high-Δ_{rms} randomized systems in Figure 3. These systems correspond to near-spherical satellite distributions $c/a > 0.8$. This tail is less prominent for simulated systems, suggesting a dearth of such near-spherical satellite systems in a full cosmological context. This result agrees qualitatively with Libeskind et al., who found that the preferential accretion of satellites from local large-scale structure naturally forms anisotropic, somewhat ellipsoidal subhalo distributions.

Similar to the spatial correlation parameters c/a and Δ_{rms}, the simulated distribution of $\angle_{rms}$ is shifted towards a stronger degree of correlation. The most kinematically correlated simulated systems in both mass regimes reach $\angle_{rms} < 40°$, while their randomized counterparts rarely achieve values of $\angle_{rms} < 45°$. The mean values of $\angle_{rms}$, 50.8° for large-bin systems and 50.3° for small-bin systems, differ from isotropy by 1.6σ and 1.4σ respectively.

Simulated $\angle_{rms}$ distributions are highly similar between mass bins, more so than c/a – a KS test yielded a 15.2% chance of being drawn from the same distribution. This

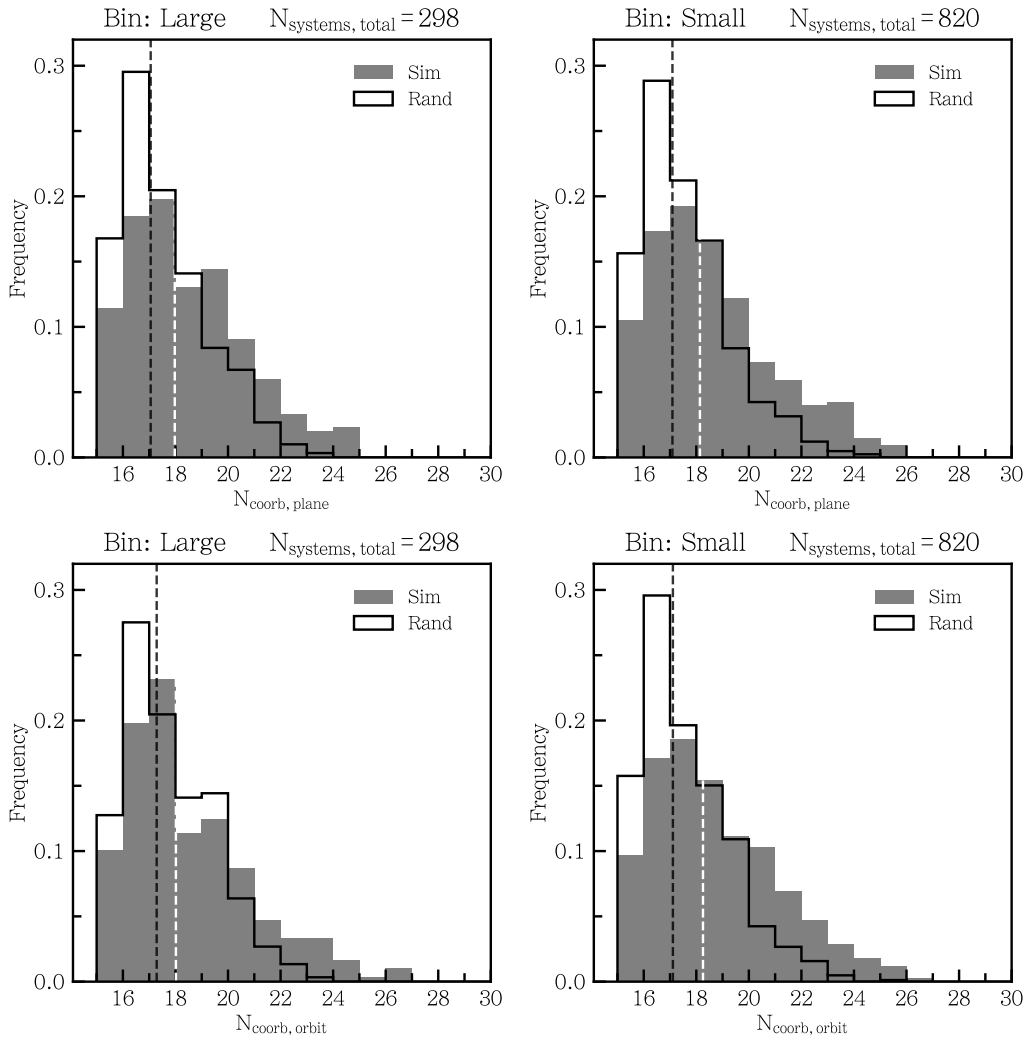

Figure 4: Distributions of $N_{coorb,plane}$ and $N_{coorb,orbit}$, the number of satellites orbiting in the same direction around the best-fit plane's normal vector or the best-fit orbital pole respectively. Simulated systems are drawn in grey, while their randomized counterparts are drawn in black outlines. White and black dashed lines indicate mean values for simulated and randomized systems respectively. Simulated systems demonstrate a stronger degree of co-rotation by a mean shift of 2 satellites.

suggests that the orbital properties of satellite systems in a cosmological context is less mass scale-reliant than their spatial properties.

Next, I consider the number of satellites co-orbiting around a system's best-fit plane normal vector $\hat{r}$ or best-fit orbital pole $\hat{p}$ (see Figure 4). As only the 30 most massive satellites are selected for systems in either mass regime, a fair comparison is possible between large-bin and small-bin systems.

The majority of both simulated and randomized systems have $16 - 20$ satellites co-orbiting along $\hat{r}$ or $\hat{p}$. The most strongly correlated simulated systems with respect to N_{coorb} may occasionally achieve co-orbiting populations of up to 26 satellites. randomized systems still achieve populations of up to 24 satellites in rare instances. Distributions of simulated $N_{coorb,plane}$ have values shifted from isotropy by 0.90 and 1.06 satellites for large-bin and small-bin systems respectively. Similarly, distributions of simulated $N_{coorb,orbit}$ have values shifted from isotropy by 0.8 and 1.1 satellites for large-bin and small-bin systems respectively.

In a distinct satellite plane, satellites are expected to preferentially orbit around the system's best-fit orbital pole $\hat{p}$. This would result in a large portion of the system's population roughly orbiting within a disk orthogonal to $\hat{p}$. On the other hand, if $\hat{p}$ was misaligned with the best-fit plane's normal vector $\hat{r}$, $N_{coorb,orbit} > N_{coorb,plane}$ is expected. Instead, distributions of $N_{coorb,orbit}$ and $N_{coorb,plane}$ are nearly identical within either mass regime (a KS test yields $p_{large} = 99.9\%$, $p_{small} = 56.4\%$). I infer that no such preference for best-fit orbital poles exist. Systems with higher co-orbiting satellite populations in Figure 4 may arise from weakly correlated satellite systems flattened along its best-fit axis of rotation.

In summary, satellites systems within a simulated ΛCDM universe at present time demonstrate a notably high degree of spatial and kinematic correlation when compared to an isotropic null-hypothesis. This degree of correlation is expected – factors such as the accretion of satellites from filaments (*e.g.* Libeskind et al.; Zentner et al.; Libeskind et al.) and larger infall events (*e.g.* Li and Helmi; Shao et al.) introduce anisotropy into halo substructure.

2.4.2 Interrelationships Between Parameters

I now test for interrelationships between a system's degree of spatial correlation and any tendency to co-rotate among its satellites. In Figure 5, the number of satellites co-rotating along the best-fit plane $N_{coorb,plane}$ is plotted against the system's degree of flattening, c/a. The upper two panels, corresponding to large-bin and small-bin simulated systems, demonstrates a large spread of systems towards higher $N_{coorb,plane}$ and lower c/a. Their randomized counterparts are concentrated in the lower right-hand corner of the lower two panels, corresponding to a low degree of phase-space correlation. There does not appear to be any visible correlation between $N_{coorb,plane}$ and c/a – using Pearson's r, there is an 18% chance for large-bin systems and a 35% chance for small-bin systems that the two parameters are fully uncorrelated.

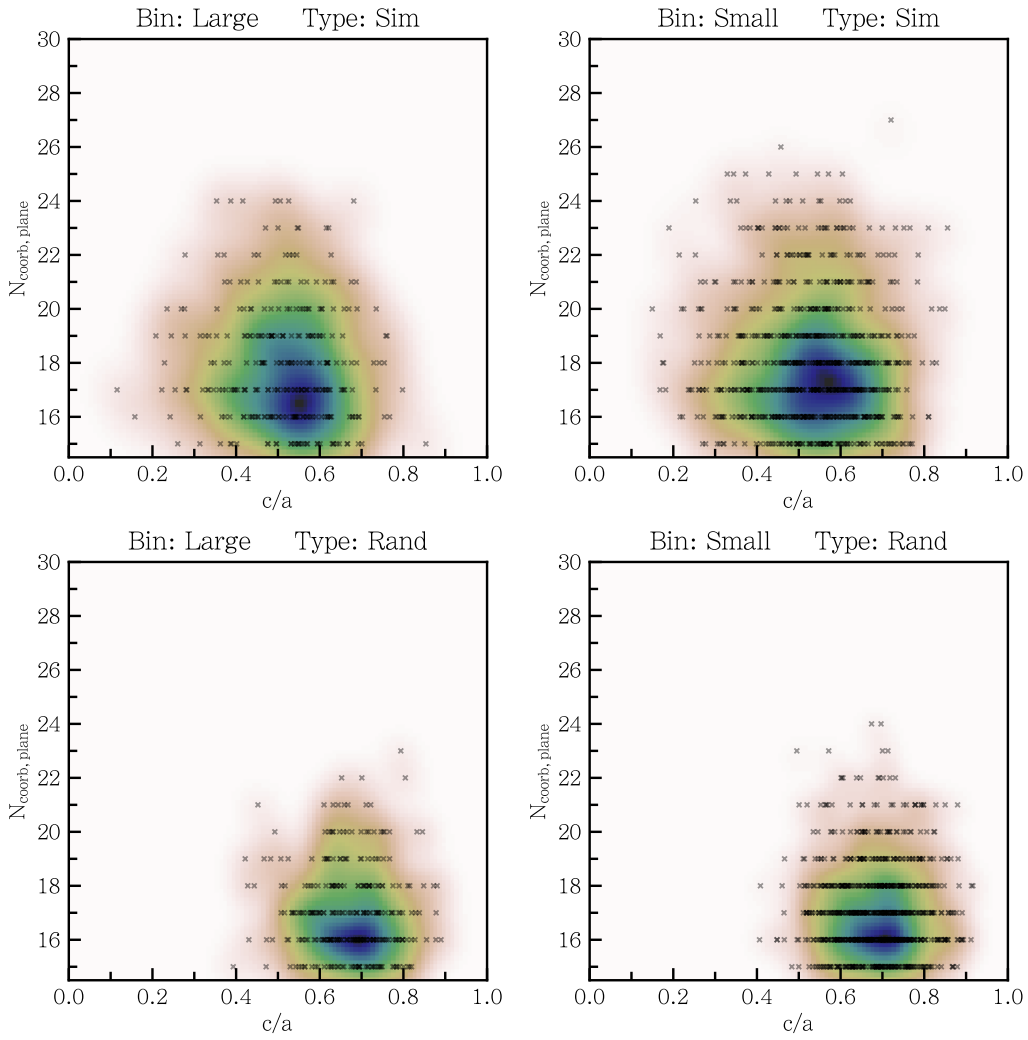

Figure 5: Overlaid scatter and density plots between $N_{coorb,plane}$ and c/a. Each system is marked with a black cross, while the underlying density plot illustrates the most concentrated area of each plot in dark blue. There is no significant correlation between a simulated system's degree of flattening and the tendency for the system's satellites to co-rotate along the best-fit plane.

Similarly, I test for correlation between $N_{coorb,orbit}$ and $\angle_{rms}$ (see Figure 6). Again, there is a smaller spread in both parameters $N_{coorb,orbit}$ and $\angle_{rms}$ for the randomized systems, with several outliers. There is a 10% chance for large-bin systems and a 7% chance for small-bin systems that the two parameters are fully uncorrelated. The lower probabilities compared to $N_{coorb,orbit}$ and c/a may be due to the concentration of systems in the low-$N_{coorb,orbit}$, high-$\angle_{rms}$ quadrant of both simulated plots.

Finally, I explore the possibility of a link between the degree of spatial flattening and kinematic correlation in sampled systems (see Figure 7). I elect to use c/a as my

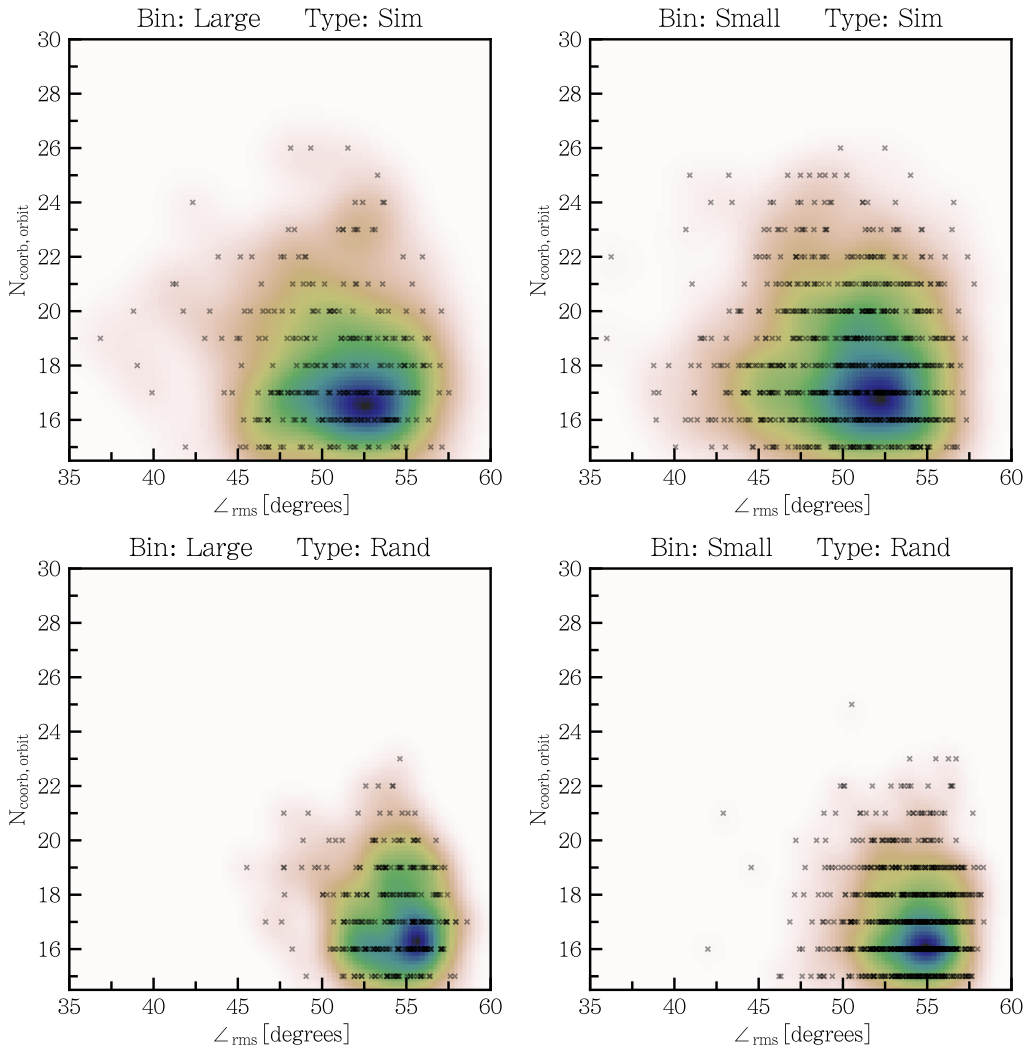

Figure 6: Same as Figure 5, but between $N_{coorb,orbit}$ and $\angle_{rms}$. There is no significant correlation between a simulated system's degree of orbital correlation and the tendency for the system's satellites to co-rotate along the best-fit orbital pole.

best measure of flattening due to its universal scale, while Δ_{rms} differs depending on the mass regime. Are highly flattened systems necessarily highly orbitally coherent?

There is a positive correlation between $\angle_{rms}$ and c/a in simulated systems (Pearson; $r = 0.334$, $p = 4 \times 10^{-9}$ for large-bin systems, $r = 0.293$, $p = 8 \times 10^{-15}$ for small-bin systems). Interestingly, a weaker correlation is also found in randomized systems (Pearson; $r = 0.178$, $p = 2 \times 10^{-3}$ for large-bin systems, $r = 0.141$, $p = 5 \times 10^{-5}$ for small-bin systems). I argue that a small degree of correlation is intrinsic, due to orbital poles containing positional information – flattened systems are expected to have an improved alignment of orbital poles to the best-fit plane's normal vector.

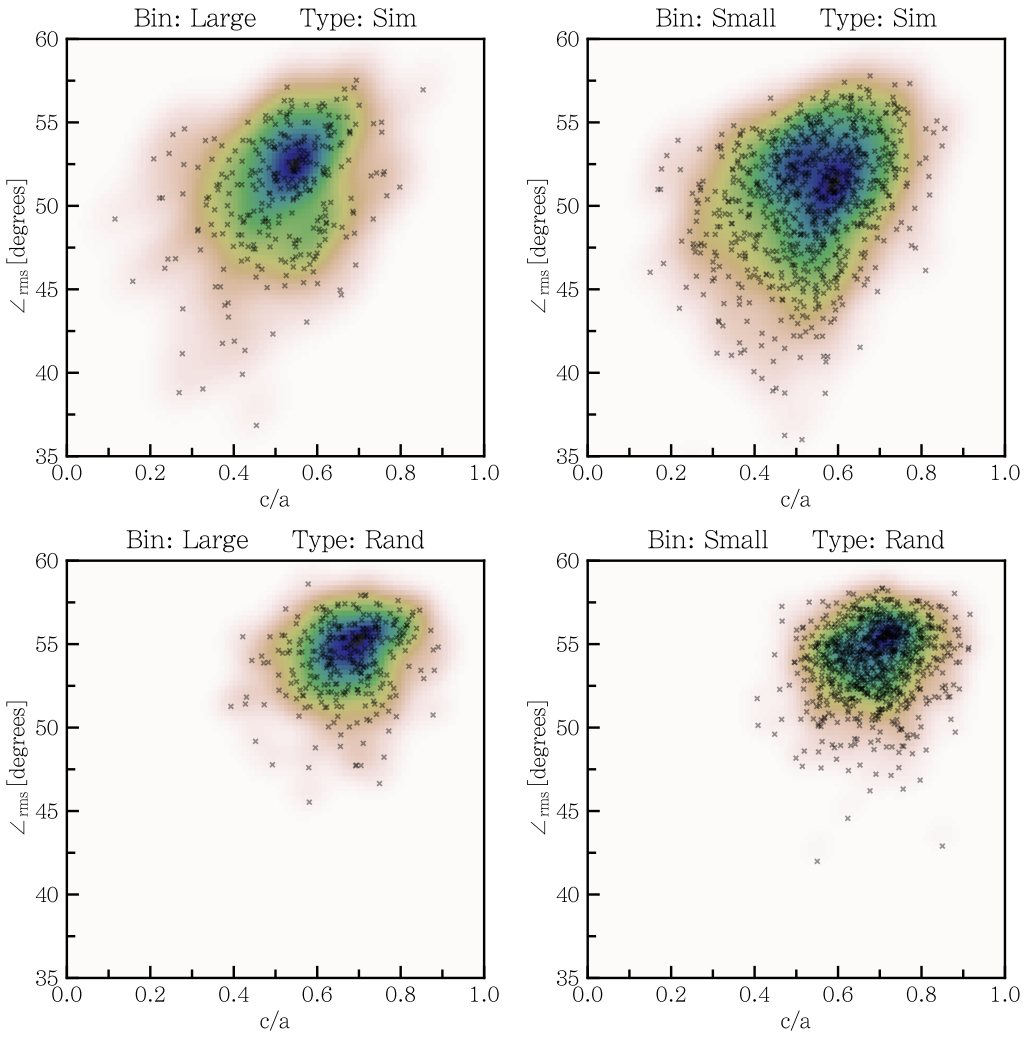

Figure 7: Same as Figure 5, but plotting each system's degree of kinematic correlation $\angle_{rms}$ against their degree of flattening c/a. Systems with near-isotropic (high c/a) satellite distributions tend to be less orbitally correlated (high $\angle_{rms}$).

However, the correlation between $\angle_{rms}$ and c/a identified in simulated systems is substantially stronger, suggesting an underlying effect.

We may visually confirm a dearth of high-c/a, low-$\angle_{rms}$ systems. There is also a limited number of systems in low-c/a, high-$\angle_{rms}$ areas. Interestingly, areas where little or no satellites are found are characterized by the distribution of outlying systems, rather than those clustered near the mean values of either parameter. Low-$\angle_{rms}$, low-c/a systems are rare, for example, but there is an even clearer lack of systems in low-$\angle_{rms}$, high-c/a areas. Additionally, there is also a noticeable dearth of systems in low-$\angle_{rms}$, low-c/a areas corresponding to highly flattened and orbitally

correlated systems. This is especially apparent with the larger sample size of small-bin simulated systems (top-right panel in Figure 7).

I argue that, to a certain extent, systems with a low degree of flattening also tend to have a low degree of orbital correlation, and vice versa. The threshold for this effect appears to be around $c/a = 0.4$ and $\angle_{rms} = 45°$, after which there is a noticeable lack of systems with strong flattening and strong orbital correlation. Thus, there is insufficient evidence to argue that flattened systems are necessarily orbitally correlated, or vice versa – on the contrary, such highly correlated systems are extremely rare.

Finally, the trends discussed above appear to be more defined for small-bin systems. This is presumably due to the greater sample size of small-bin systems (820) than large-bin systems (298). As discussed in Section 2.4.1, the individual distributions of c/a and $\angle_{rms}$ are highly similar between the two mass regimes. In the absence of any other evidence, I suggest that both small-bin and large-bin systems demonstrate a similar degree of correlation between spatial and kinematic parameters.

3 Comparisons With Merger History

In Section 2, I found that highly spatially or kinematically correlated satellite systems are rare around M31 and Centaurus A-mass host galaxies at present time. In this section, I consider the individual merger histories of each system to ascertain whether the existence of a recent merger influences the degree of phase-space correlation in their satellite distribution.

3.1 Classifying Merger History

The merger history of each satellite system – or more precisely, that of two merging centrals – was classified for analysis. I define a major merger as a merger where two centrals interact with a dark matter subhalo mass ratio of 1:3 or higher. As discussed in Section 1.5, mergers with lower mass ratios are unlikely to form richly populated satellite planes. I call the more massive participating central the *primary central*, belonging to the *primary halo* before the merger occurs. Similarly, I call the less massive participating central the *secondary central*, belonging to the *secondary halo* before the merger occurs.

Mergers were traced using IllustrisTNG's Sublink merger catalog (Rodriguez-Gomez et al.). In Sublink, mergers are defined by whether a subhalo has more than one progenitor subhalo in the previous snapshot. If so, two subhaloes must have merged to form their descendant in the current snapshot. I define the time at which a merger occurs as the first snapshot where the two progenitors are recognized as a single subhalo by Sublink. This snapshot is called the merger's *end* snapshot.

Before a merger event, mass is usually accreted from the secondary central by the primary central. This leads to the secondary central retaining only a minimal amount of mass at the snapshot before the two centrals merge. Thus, I used the maximum mass each subhalo had in the past to determine the mass ratio of any given merger. For near-1:1 mergers, this method occasionally caused a discrepancy between the direction of mass accretion between the two centrals and the maximum past masses of the two centrals. This discrepancy resulted in mergers with mass ratios above 1:1. In such rare cases, the primary and secondary designations were flipped. Only mergers where two progenitor subhaloes had maximum past dark matter masses in a 1:3 ratio or above were considered. When merger ratios are displayed as single values, the inverse ratio is shown – a 1:3 ratio, for example, is indicated as $r_{merger} = 3$.

System Type	Criteria	N_{large}	N_{small}
Merger	Major merger within last 11 Gyr	103	176
Quiescent-type	No major mergers within last 5 Gyr	251	741
Merger-type	Major merger within last 5 Gyr	44	64
Recent	Major merger within last 2 Gyr	13	20

Table 1: Merger history classification criteria for centrals in selected systems.

In this study, only the last major merger that a given system has experienced was considered. Each new merger event is expected to imprint a new angular momentum vector into the system. Thus, a system's last major merger should have a dominant effect on its current satellite distribution. I additionally rejected all systems where the second-last major merger occurred within 5 snapshots (0.5 Gyr) of the last major merger. Such systems may be too chaotic to analyse an individual merger event's impact on satellite distributions. 295 large-bin systems and 805 small-bin systems passed this criterion.

All remaining systems were divided into the following categories. I define *quiescent-type* systems as those which have not experienced any major mergers after snapshot 68, or within the last 5 Gyr. I define *merger-type* systems as those with at least one major merger after snapshot 68. Additionally, I define *recent* systems as a subset within *merger-type* systems – these have at least one major merger after snapshot 87, or within the last 2 Gyr. These classification criteria are also shown in Table 1.

The motivations for these criteria are as follows. Smith et al. reported that in their idealized model, generated satellite planes had lifetimes of 6 Gyr or more. If this is also the case in a full cosmological context, *merger-type* systems with the correct initial conditions should host satellite planes. On the other hand, mergers may form satellite planes that are short-lived instead. To test this, I selected a timespan of around 2 Gyr for *recent* systems. Smith et al. found that lopsidedness from mergers took around $1 - 1.5$ Gyr to stabilize. Thus, systems with mergers within 2 Gyr should still demonstrate a skewed satellite distribution even if the formed plane is intrinsically short-lived.

Finally, I define a set of *merger* systems, which includes all systems with at least one major merger after snapshot 30, or within the last 11 Gyr. This serves as my working sample of systems when considering any potential correlation between correlation parameters at present time and and the properties of a system's last major merger. It is not useful to consider systems without any major mergers within such a reasonably large timespan.

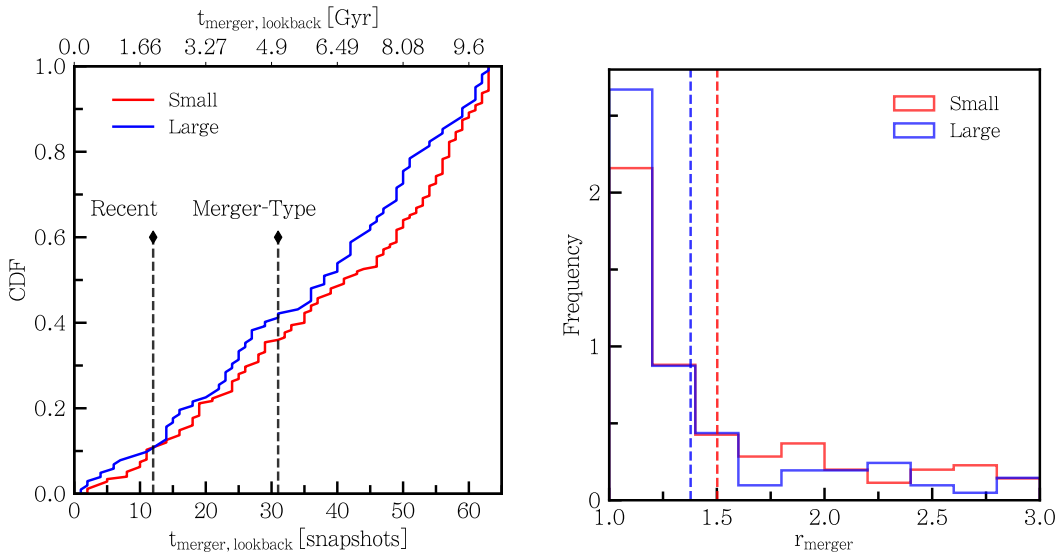

Figure 8: *Left Panel:* CDF for last merger end-point lookback times for all simulated systems with mergers above a mass ratio of 1:3 within 11 Gyr. The distribution for small-bin and large-bin systems are drawn in red and blue respectively. Threshold times for designating a merger as *recent* or *merger-type* is shown in black, corresponding to $\approx$ 2 Gyr and 5 Gyr respectively. *Right Panel:* Merger ratios of all systems with major mergers within 11 Gyr. Mean values for small-bin and large-bin systems are drawn in red and blue dashed lines respectively.

Figure 8 shows the distribution of merger ratios and lookback times for the last major mergers of sample systems. The number of last mergers ending between present time and 11 Gyr ago is roughly evenly distributed for large-bin systems, while small-bin systems appear to be skewed towards earlier mergers.

This suggests that M31 or Milky Way-mass centrals, corresponding to small-bin systems, tend towards a generally violent early history from the hierarchical clustering of subhaloes in ΛCDM followed by a period of relatively quiescent growth. On the other hand, while many large-bin *merger* systems have also experienced quiescent growth after early major mergers, there is a consistent population that continue to experience major mergers up to present time.

The right-hand panel in Figure 8 plots the distribution of merger ratios of each system's last major merger. Interestingly, most mergers in both mass regimes demonstrate near-1:1 mass ratio. The fraction of systems with near-1:1 mergers is slightly higher for large-bin systems.

3.2 Impact on Satellite Distributions

I now investigate the impact of major mergers on correlation in satellite distributions. The distributions of the three correlation parameters c/a, Δ_{rms}, and $\angle_{rms}$ are shown separately for *quiescent-type*, *merger-type*, and *recent* systems in Figure 9.

I initially consider the impact of mergers on c/a distributions. The spread of c/a for *quiescent-type* and *merger-type* systems appears similar for large-bin systems, with nearly identical median values at a 0.015 shift. A KS test yielded a 73.1% chance that the two are drawn from the same distribution – the existence of a major merger in the last 5 Gyr does not appear to influence flattening on average. Distributions for *quiescent-type* and *merger-type* systems are similar for small-bin systems, but there is a slight shift towards higher c/a – and analogously a less flattened satellite distribution – for *merger-type* systems. The median values are still nearly identical, however, at a 0.003 shift.

The c/a distribution for *recent* systems is also highly similar to that of *quiescent-type* systems, with negligible median c/a shifts in either mass regime. Interestingly, the *recent* c/a distribution for large-bin systems appears to be centrally concentrated – this feature is not prominent for small-bin systems. However, with a sample of only 13 large-bin *recent* systems, this could also be a result of small-sample error.

Results are similarly inconclusive when considering Δ_{rms} as a metric of plane flattening for *quiescent-type* and *merger-type* systems. For large-bin systems, the mean Δ_{rms} for *merger-type* systems is raised by 6 kpc from that for *quiescent-type* systems. This shift is smaller still for small-bin systems. On the other hand, mean Δ_{rms} is visibly higher for *recent* systems when compared to *quiescent-type* for both mass regimes. Specifically, *recent* systems demonstrate a mean shift of 0.6σ and 0.4σ towards a thicker plane for large-bin and small-bin systems respectively. Here, the presence of a major merger in the last 2 Gyr appears to reduce the degree of flattening for the resultant present-time satellite distribution.

This weakening in phase-space correlation after a recent merger is also apparent when considering the orbital properties of the sampled systems. The $\angle_{rms}$ distribution for *recent* systems, and *merger-type* systems to a lesser extent, are centrally concentrated when compared to *quiescent-type* systems. There is a reduction in the low-$\angle_{rms}$ population for *recent* and *merger-type* systems. This is reflected in the mean $\angle_{rms}$ for each system type, with *recent* systems deviating from the *quiescent-type* distribution by 0.3σ and 0.4σ for large-bin and small-bin systems respectively. On average, recent merger activity appears to slightly reduce the degree of kinematic

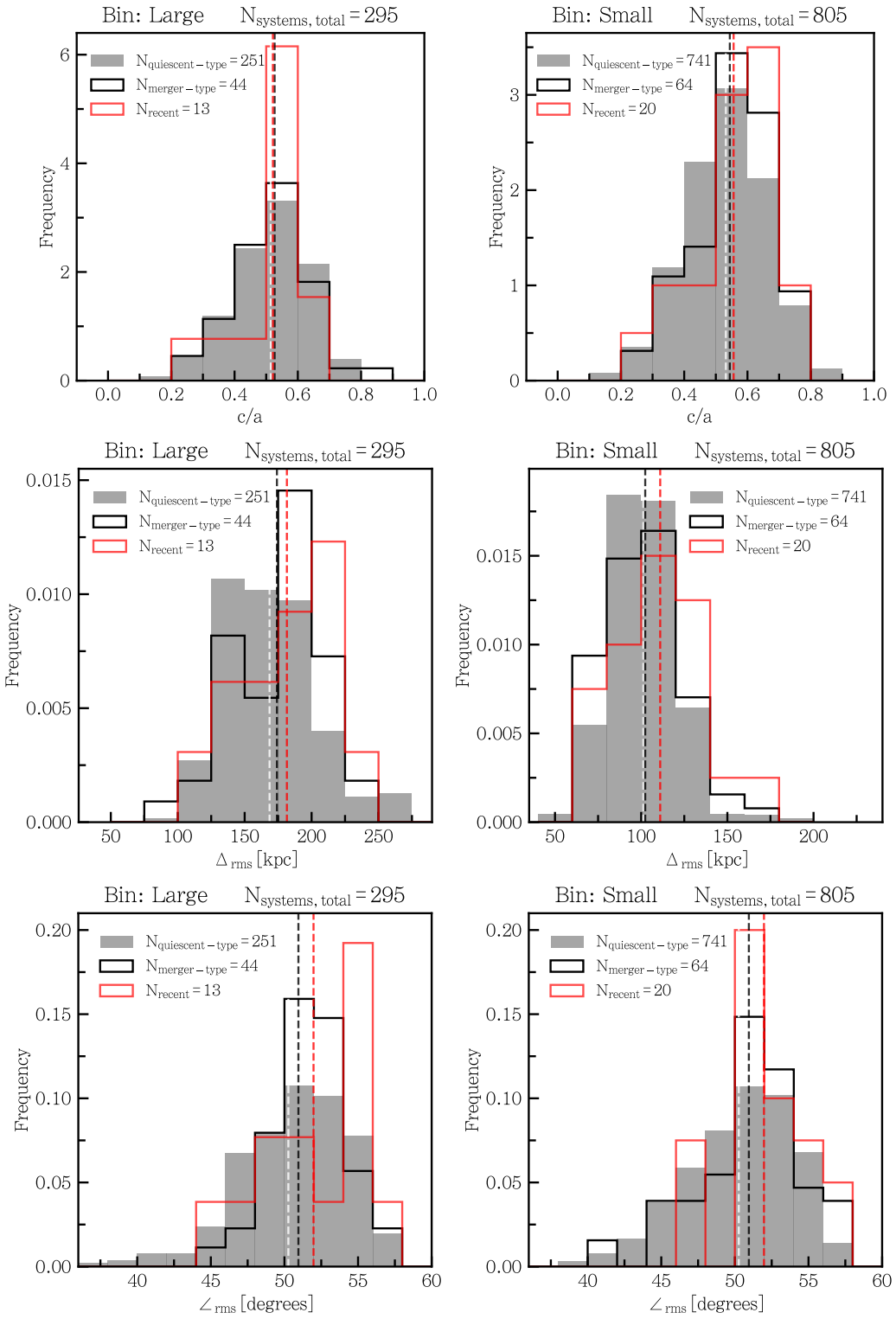

Figure 9: Correlation parameter distributions for systems categorized by their merger history. *Quiescent-type* systems are drawn in gray, while *merger-type* and *recent* systems are indicated in black and red outlines respectively. White, black and red dashed lines indicate the mean values of each respective distribution. A more recent merger appears to be weakly linked to a lower degree of phase-space correlation.

		$t_{lookback}$		r_{merger}	
Parameter	Mass Regime	r	p (%)	r	p (%)
c/a	Large	-0.028	77.5	-0.077	43.4
c/a	Small	0.028	71.5	-0.010	89.2
Δ_{rms}	Large	-0.130	18.7	0.099	31.4
Δ_{rms}	Small	-0.081	28.1	-0.155	3.9
$\angle_{rms}$	Large	-0.064	52.1	-0.048	62.9
$\angle_{rms}$	Small	-0.137	6.9	0.115	12.5

Table 2: Pearson correlation coefficients and p-values from testing the relationship between c/a, Δ_{rms}, $\angle_{rms}$ and merger end-point lookback time, mass ratio for the two mass regimes.

correlation for sampled satellite systems. However, the small shifts found are by no means conclusive.

The classification of systems into discrete categories based on their merger history has the benefit of considering all sampled systems, including systems without any major mergers recorded within the last 11 Gyr. We may also directly consider potential correlations between the three correlation parameters c/a, Δ_{rms}, and $\angle_{rms}$ and two properties of each system's latest merger – the lookback time to their merger's end point t_{merger} and their merger's mass ratio r_{merger} (see Figure 10). This data can also be found in Table 2.

It is important to note that this approach only considers *merger* systems, which have experienced one or more major mergers within the last 11 Gyr. On the other hand, we are able to test for direct correlations between merger properties and those of the resultant present-time satellite distribution by constraining our sample.

Other than a slight negative correlation between Δ_{rms} and r_{merger} for small-bin systems, none of the tested relationships provide any statistically significant evidence for correlation. Visually, it appears that the rolling mean of Δ_{rms} is higher for systems with major mergers within ≈ 4 Gyr of present time. However, there is also a consistent population of more flattened systems throughout this period – this data does not conclusively show that recent mergers increase plane height.

Certain areas demonstrate an unusually low population of systems, which may not be fully represented in the r-values in Table 2. Specifically, there is a visual dearth of systems with low $\angle_{rms}$ with a recent merger (corresponding to a low t_{merger}). If not a small-sample anomaly, this may suggest that recent mergers (approximately within 2 Gyr) prevent the formation of highly kinematically correlated systems. It

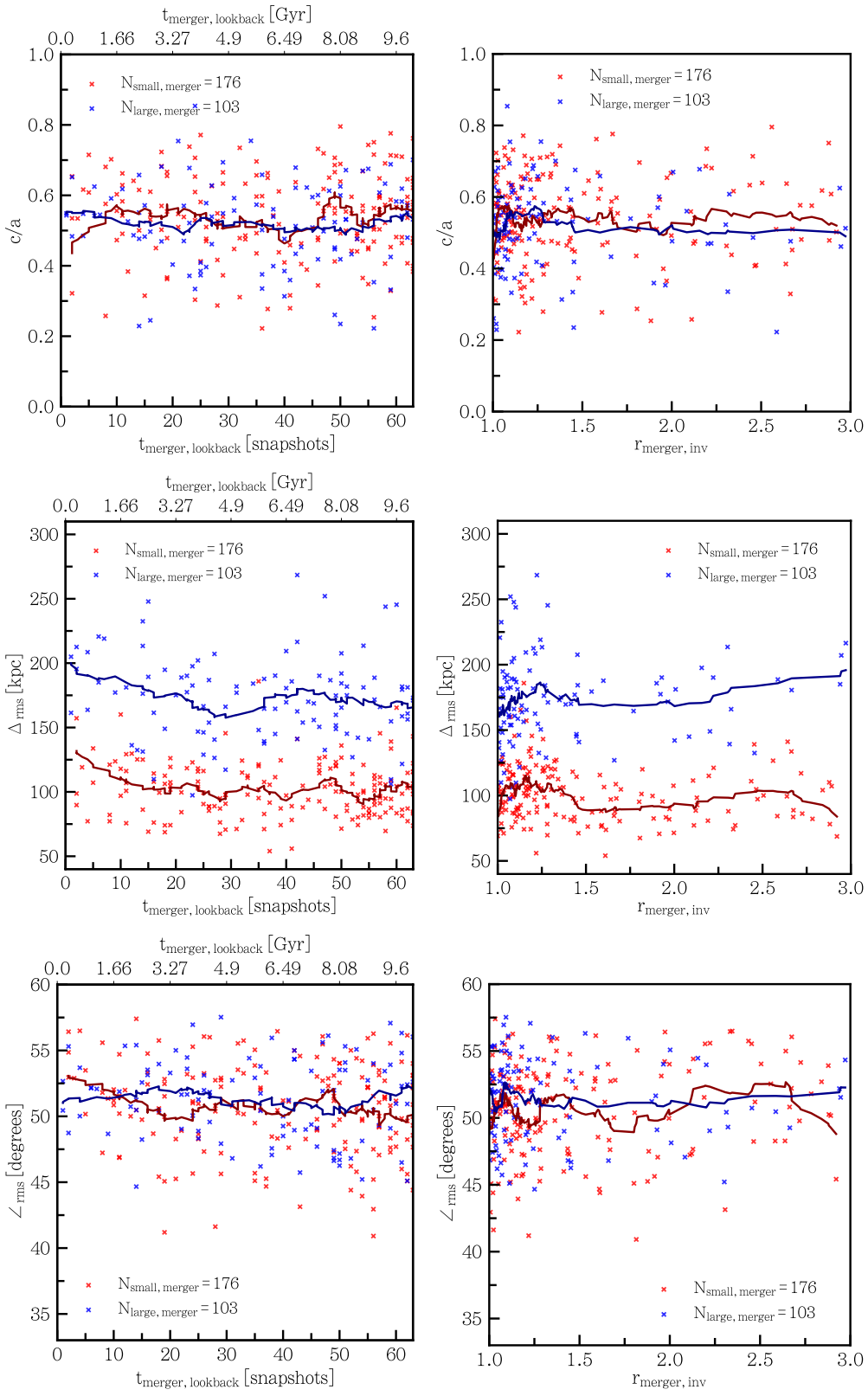

Figure 10: Correlation parameters c/a, Δ_{rms}, $\angle_{rms}$ plotted against the lookback time and mass ratio of sampled *merger* systems' last major mergers. A rolling mean across 20 data points along the x-axis is drawn in dark blue and dark red.

appears that merger ratio does not influence the degree of correlation in satellite systems to any significant degree.

Overall, results from Figure 9, Figure 10, and Table 2 indicates that recent major mergers appear to have a negligible impact on satellite phase-space correlation at present time. Some data may suggest that mergers may decrease the degree of correlation in satellites, but is insufficient to argue so convincingly. This stands in contrast to the initial expectations, where mergers aid in the formation of highly correlated satellite distributions. I find no significant evidence that merger events form correlated satellite distributions.

3.3 Tracking Merger Trajectories

In the previous section, I tested whether recent merger events in general influence the phase-space correlation in satellite systems, and the role of a merger's recency and mass ratio. However, in Smith et al.'s model of satellite plane formation, specific requirements are imposed on a merger's properties. Merger recency and mass ratio have already been considered. In this section, I investigate the role of a merger's infall trajectory on its ability to influence resultant satellite distributions.

Firstly, I determine the beginning of each merger, which is a point in time where the two centrals involved are gravitationally bound and will inevitably merge, but prior to any strong gravitational influence being placed on the participating satellite distributions by the opposing centrals. Smith et al. defined the beginning as when the centre of the secondary halo is located at the virial radius of the primary halo. However, the merger would have already progressed considerably when this occurs, as the satellite population of both haloes would have overlapped. I instead define the beginning – which is referred to as the *start* point in this dissertation – as the last snapshot before the distance between the two participating centrals is equivalent to the sum of their haloes' virial radii. If two centrals are already bound to the same halo at this time, I doubled that halo's virial radii to determine the threshold distance.

Next, I define the key parameters that describe the infall trajectory and orientation of a merger event. To recognize mergers with circular or radial infall trajectories, Smith et al. calculated the magnitude of the tangential orbital velocity of the two participating centrals if it was a stable, Newtonian two-body system. However, this definition assumes that both centrals lack radial velocity components at the

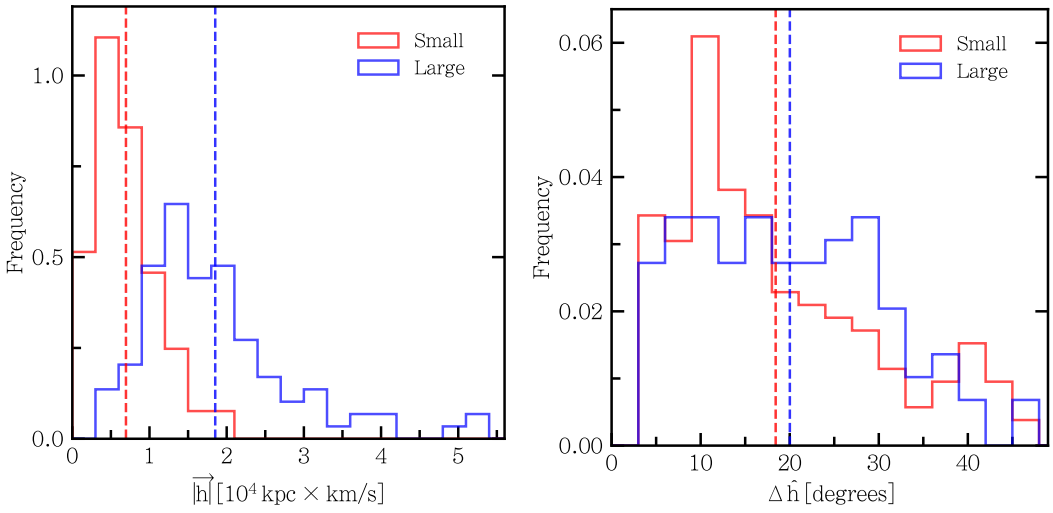

Figure 11: Distributions of the summed merger specific angular momentum $|\vec{h}|$ and stability $\Delta\hat{h}$. Small-bin and large-bin systems are drawn in red and blue outlines, while their mean values are drawn in red and blue dashed lines.

beginning of their merger, which is unrealistic in a full cosmological context. Instead, I describe the nature of a merger's infall trajectory using the summed specific angular momentum $\vec{h}$ of the two centrals. Its magnitude, $|\vec{h}|$, should be higher for circular infall trajectories and lower for radial infall trajectories.

The orientation of the merger's total specific angular momentum $\vec{h}$ also defines the approximate plane in which the merger occurs. Thus, $\hat{h}$ can be referred to as the *merger axis*, which characterizes the *merger plane*. I also define a merger's *duration* as the number of snapshots (or length of time) between its start and end points.

As the two centrals fall towards each other, their angular momentum decreases due to dynamical friction. Thus, $|\vec{h}|$ changes over the course of a merger. Its earlier values are most representative of a merger's initial trajectory. Thus, I take the average $|\vec{h}|$ over the first 50% of the merger's duration, rounded up if the duration is an odd number of snapshots.

Similarly, mergers do not occur in a perfectly stable plane. External forces and torques will modify $\hat{h}$ over time. As the radial distances of the two centrals from the merging system's barycentre grows smaller, the direction of $\hat{h}$ may flip – the rotational direction of the centrals with respect to the barycentre is effectively reversed. I found that $\hat{h}$ tends to be stable during the early stages of the merger, losing stability as the merger progress. Thus, I calculated the RMS spread of $\hat{h}$ over the first 50% of a merger's duration, rounded up if it is an odd number of snapshots. As $\hat{h}$ reversals do not necessarily imply a chaotic merger, I consider opposing $\hat{h}$ vectors

identical. Thus, its RMS spread – a useful indicator of merger stability – is limited to $0° \leq \Delta\hat{h} \leq 90°$.

The upper panels in Figure 11 show the distribution of $|\overrightarrow{h}|$ and $\Delta\hat{h}$ for both mass regimes. Large-bin systems tend towards higher $|\overrightarrow{h}|$, an expected result of higher central masses. Both large-bin and small-bin systems appear to follow a similar $|\overrightarrow{h}|$ distribution, though small-bin systems lack the "tail" at higher $|\overrightarrow{h}|$ that is seen for large-bin systems.

The upper right-hand panel, which shows the distributions of $\Delta\hat{h}$, is more ambiguous. In both mass regimes, a majority of systems have values of 30° or less, with a mean $\Delta\hat{h}$ of around 20°. There is a lower number of small-bin systems with $20° < \Delta\hat{h} < 35°$, while demonstrating a high peak at $\approx 12°$. This may suggest that mergers at smaller mass scales are more stable.

3.4 Trajectories and Satellite Correlation

I now consider the alignment between a major merger's axis, $\hat{h}$, and the resultant present-time satellite distribution's best-fit plane normal vector or orbital pole for all *merger* systems (see Figure 12).

If the orientation of plane flattening or orbital cohesion is strongly influenced by mergers, $\hat{h}$ should be well-aligned with either. However, strong alignments of $< 20°$ are rare in both mass regimes, only occurring in around 10% of systems. When compared to the distribution of alignments between two randomly oriented vectors, $\hat{h}$ appears to somewhat preferentially align with the best-fit orbital pole, $\hat{p}$. This effect is weaker for alignments with the best-fit plane normal, especially for small-bin systems. In general, mergers may have a noticeable influence on the orbital direction of resultant satellite populations. This does not necessarily correspond to highly correlated orbits, however – Figure 9 and Figure 10 do not demonstrate any major increase in the kinematic correlation of satellites. The enhancement in alignment between $\hat{h}$ and $\hat{p}$ may also result from preferential accretion of satellites along the merger plane before the merger began.

Next, I investigate whether a merger's stability $\Delta\hat{h}$ is linked to its trajectory via its summed specific angular momentum, $|\overrightarrow{h}|$ (see lower panel, Figure 13). Visually, we find a lower population of systems in the high-$\Delta\hat{h}$, high-$|\overrightarrow{h}|$ region. This is reflected in small but statistically significant negative correlations, especially notable for large-bin systems (Pearson; $r = -0.371$, $p = 0.015\%$ for large-bin systems, $r =$

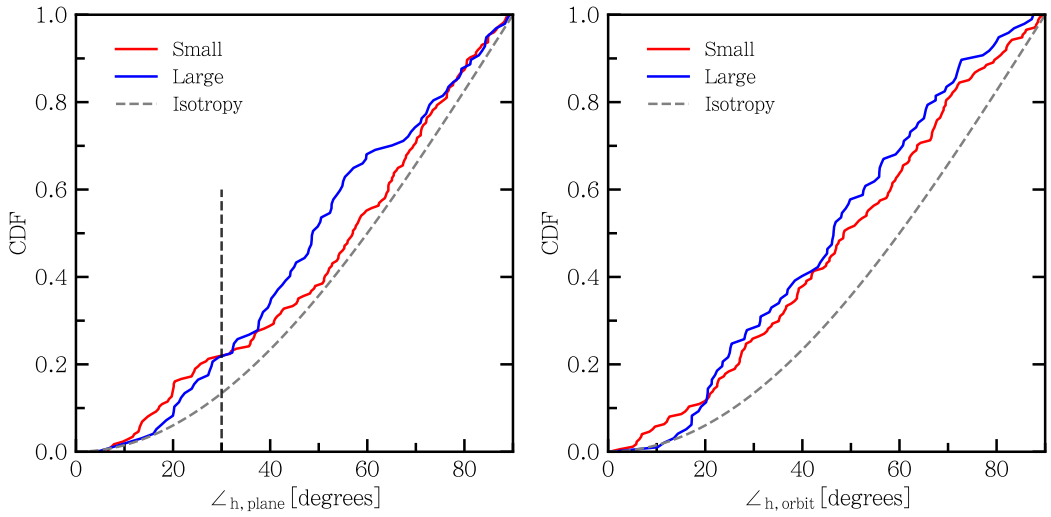

Figure 12: CDFs of the alignment between merger axis $\hat{h}$ and the present-time system's best-fit plane normal vector or best-fit orbital pole. The alignment expected between two randomly oriented vectors are drawn in gray dashed lines. The 30° threshold for well-aligned mergers used in Figure 14 is drawn in black dashed lines. Both small-bin and large-bin systems are generally better-aligned than isotropic distributions.

-0.226, $p = 0.26\%$ for small-bin systems). This suggests that a large initial angular momentum – corresponding to a near-circular infall trajectory – tends to result in a more stable merger plane. There are many systems in Figure 13 that achieve a high degree of merger stability without a large initial $|\overrightarrow{h}|$, but it is interesting to note that mergers with high $|\overrightarrow{h}|$ generally result in relatively stable mergers with $\Delta\hat{h} < 30°$.

The upper panels in Figure 13 plots stability $\Delta\hat{h}$ against the alignment between $\hat{h}$ and the best-fit orbital pole $\hat{p}$ or plane normal vector $\hat{r}$. While no immediate correlation can be recognized, there appears to be a smaller population of systems in low-$\angle_{h,plane}$ or $\angle_{h,orbit}$, high-$\Delta\hat{h}$ regions. This is mainly relevant for small-bin systems (Pearson; $r = 0.228$, $p = 0.23\%$ for $\hat{r}$-alignment, $r = 0.282$, $p = 0.014\%$ for $\hat{p}$-alignment), while no statistical correlation is found for large-bin systems ($p = 21.8\%$ for $\hat{r}$-alignment, $p = 64.6\%$ for $\hat{p}$-alignment). This data indicates that small-bin systems may be more easily aligned with the direction of angular momentum imprinted from a merger. Alternatively, this may be a result of the larger sample size of small-bin systems, which naturally demonstrates a higher significance when compared to the smaller sample size of large-bin systems.

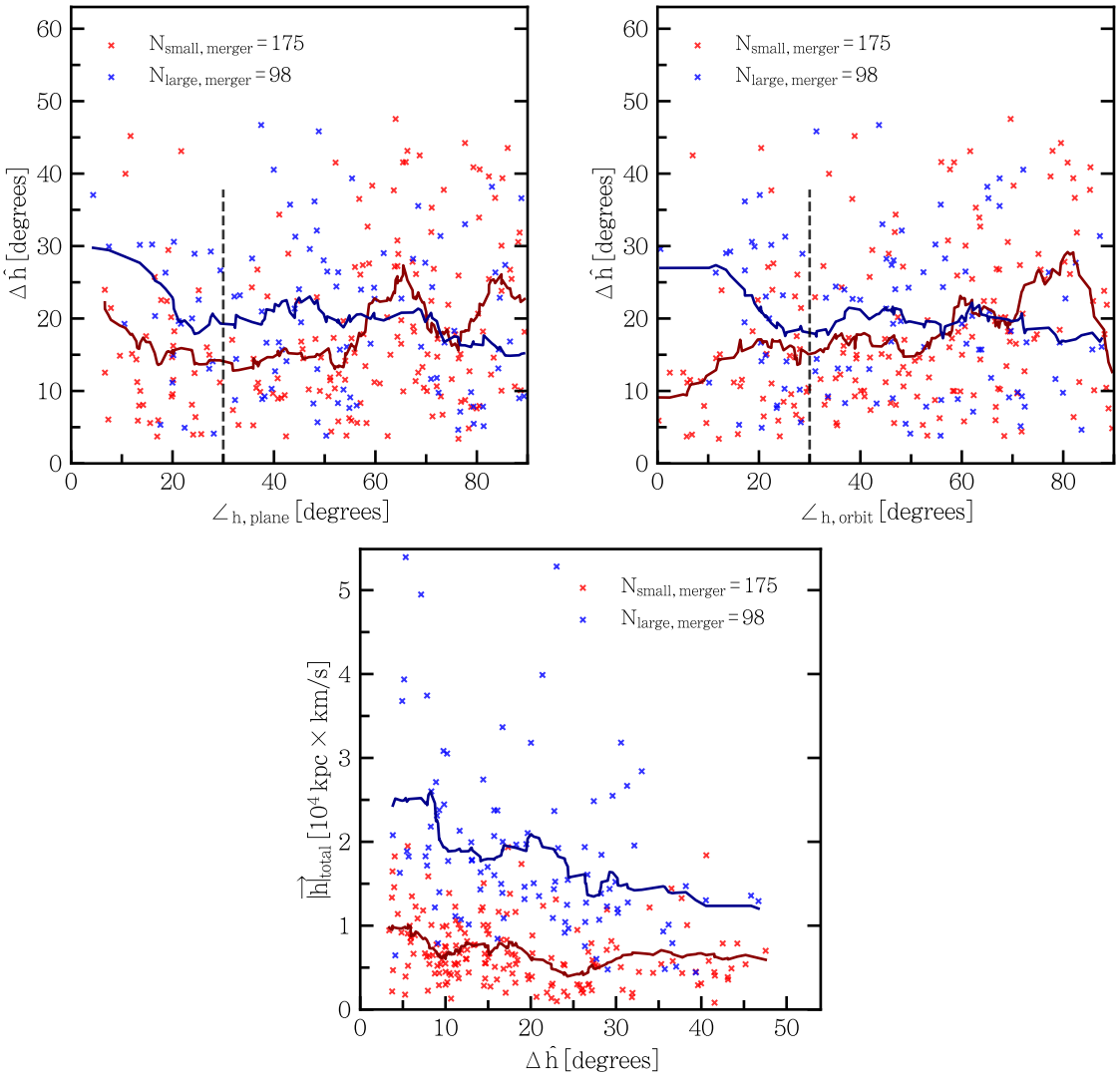

Figure 13: *Upper Panels:* Scatter plots of merger stability against the alignment angle between merger axis $\hat{h}$ and the resultant best-fit plane normal vector or orbital pole. A rolling mean across the 20 closest data points along the x-axis is drawn in dark red and dark blue for small-bin and large-bin systems respectively. *Lower Panel:* Plot of merger specific angular momentum against merger stability. Mergers with a higher specific angular momentum tend to result in more stable merger planes, which in turn is weakly linked to a better alignment.

Finally, I attempt to quantify the impact of mergers on satellite distributions in the case where $\hat{h}$ is well-aligned with $\hat{r}$ or $\hat{p}$. I argue that in such a scenario, mergers should have had the largest possible impact on the final satellite distribution, efficiently imprinting its angular momentum on the system. To do this, I separate all *merger* systems into *well-aligned* systems with an alignment of $\angle_h \geq 30°$ and *less-aligned* systems with $\angle_h \leq 30°$. We use $\angle_{h,plane}$ when considering c/a or Δ_{rms}, and

Parameter	Mass Regime	z (σ)	p (%)
c/a	Large	0.5	3.2
c/a	Small	0.3	5.5
Δ_{rms}	Large	0.4	37.1
Δ_{rms}	Small	0.3	27.0
$\angle_{rms}$	Large	0.5	10.6
$\angle_{rms}$	Small	0.5	4.3

Table 3: Degree to which correlation parameter distributions differ between well-aligned systems, where the merger axis aligns to within 30° to the resultant satellite distribution's best-fit plane normal vector (for c/a, Δ_{rms}) or best-fit orbital pole (for $\angle_{rms}$), and less-aligned systems where alignment is above 30°. KS-test z-values and probabilities that the distributions are identical are recorded.

$\angle_{h,orbit}$ when considering $\angle_{rms}$. The distribution of the three correlation parameters c/a, Δ_{rms}, and $\angle_{rms}$ for well-aligned and less-aligned systems is shown in Figure 14.

For all three correlation parameters over both mass regimes, the well-aligned systems appear to demonstrate a stronger degree of phase-space correlation, corresponding to lower values of c/a, Δ_{rms}, and $\angle_{rms}$. The results of applied KS tests, indicating the degree to which the distributions of well-aligned and less-aligned systems differ, are shown in Table 3.

The shift in distribution between well-aligned and less-aligned systems appear to be most significant for c/a, with only a $3-5\%$ chance that they are identical. The mean values of each distribution show a c/a shift of 0.056 for large-bin systems and 0.049 for small-bin systems. Despite a similarly noticeable shift in mean values for Δ_{rms}, there is a 27% and 37% chance that the two distributions are identical for large-bin and small-bin systems respectively.

A substantial decrease in c/a, along with a less notable decrease in Δ_{rms}, suggests that well-aligned mergers may induce stronger-than-average flattening through an increase in radial extent – this data agrees with Smith et al., who argued that the slinging out of satellites strongly contributes to satellite plane formation. However, unlike systems in Smith et al., well-aligned systems only marginally strengthens flattening. Additionally, the minimum c/a found for well-aligned and less-aligned systems are nearly identical. While the slinging of satellites may generally strengthen spatial correlation, it does not necessarily produce highly flattened systems.

Interestingly, the data in Figure 14 contrasts with previous findings in Section 3.2, where c/a is generally unaffected or is slightly increased by recent mergers. In Section 3.2, results were taken for all *merger-type* or *recent* systems regardless of their

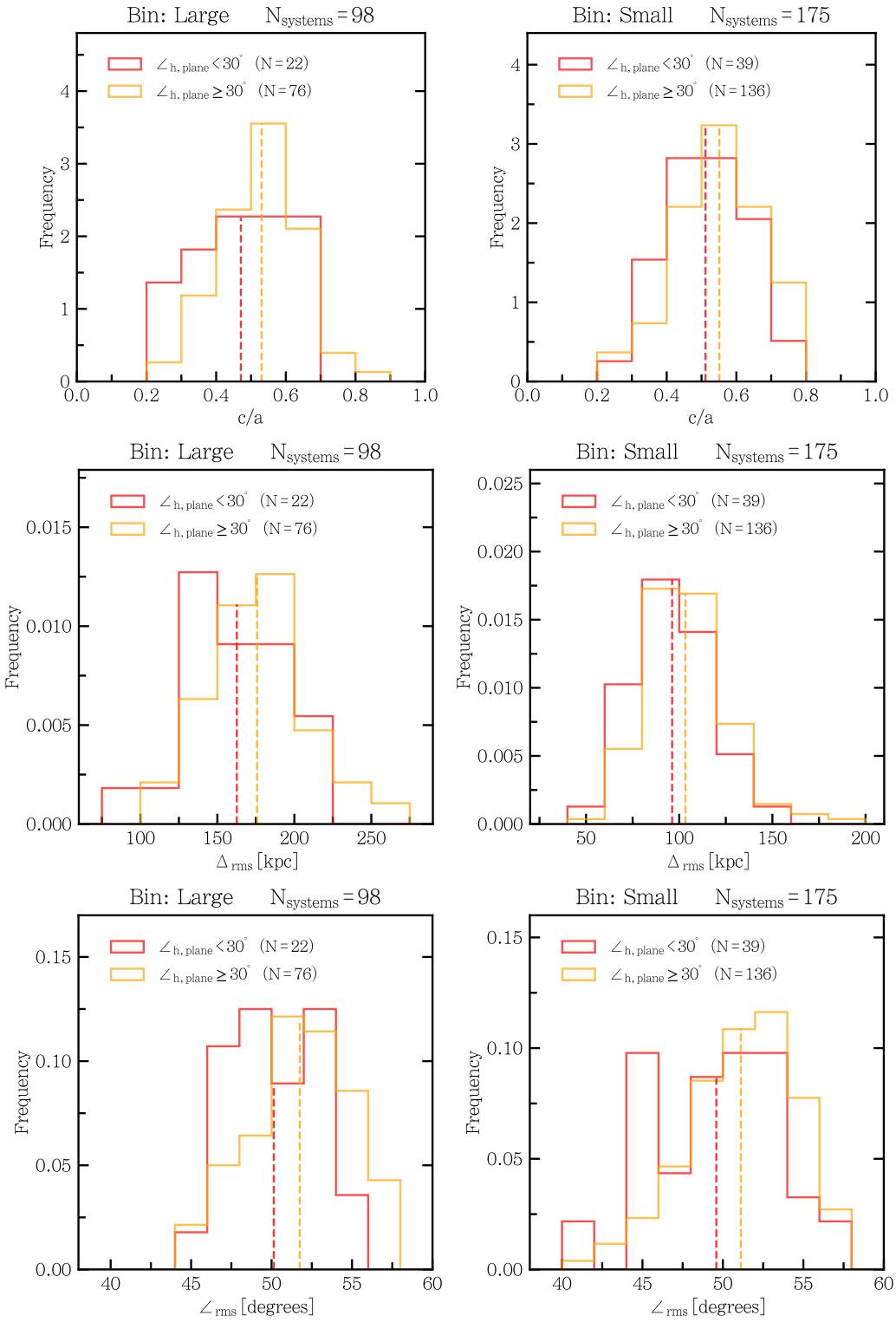

Figure 14: Distribution of correlation parameters for all *merger* systems, separated by whether their best-fit plane normal vector or orbital pole is aligned to the merger axis $\hat{h}$ by more or less than 30°. Mean values are drawn in red and orange dashed lines for well-aligned and less-aligned systems respectively. A better alignment is linked to a stronger degree of phase-space correlation for all three parameters.

$\hat{h}$-alignment. I argue that while mergers appear to weaken correlation in satellites, or else has a negligible effect, well-aligned mergers that successfully imprint their angular momentum onto the resultant satellite distributions can slightly improve spatial correlation.

Finally, I consider a merger's $\hat{h}$-alignment with the resultant satellite distribution's best-fit orbital pole and its impact on kinematic correlation (see lowest panels in Figure 14). Visually, well-aligned systems are shifted towards lower $\angle_{rms}$ and thus stronger correlation. Once again, the minimum $\angle_{rms}$ achieved for well-aligned and less-aligned systems are similar – while well-aligned mergers generally strengthen kinematic correlation, they do not generate satellite systems with highly correlated orbits.

In summary, I find that a more circular central infall trajectory tends to stabilize merger planes. A more stable merger is weakly linked to a better alignment between a merger's angular momentum vector and the best-fit plane normal vector or best-fit orbital pole of the resultant present-time satellite distribution. A well-aligned merger, in turn, appears to slightly strengthen the degree of spatial and kinematic correlation in satellite systems. However, well-aligned mergers do not preferentially produce highly correlated systems. Furthermore, this effect is minor, and is easily washed out when considering the entire set of systems with recent mergers. Only around $20 - 25\%$ of systems with major mergers within the last 11 Gyr are well-aligned, and instances where mergers improve correlation may be the exception rather than the rule. On average, mergers have a negligible or slight weakening effect on satellite phase-space correlation. This appears to be the case for systems in both sampled mass regimes.

4 Satellite Merger Participation

4.1 Participation In Sampled Systems

In previous sections, I reported that mergers only have a minor impact on satellite distributions at present time. This remained the case even when constraining our sample to well-aligned systems or those with very recent mergers. This lack of influence may be due to a substantial fraction of the present-time satellite population falling into the system after the last major merger ended.

In Section 3.2, I found that *recent* systems with a major merger within the last 2 Gyr displayed higher Δ_{rms} and $\angle_{rms}$ values than *merger-type* or *quiescent-type* systems. On one hand, this may simply reflect the short-lived nature of the merger's imprint on the system, which weakens over the course of several Gyr. Alternatively, this may be explained by *recent* systems at present time having a larger fraction of satellites that participated in and were directly influenced by the last merger. This fraction is expected to be lower for *merger-type* systems, and lower still for *quiescent-type* systems as more satellites are accreted from the surrounding post-merger environment. In this study, I refer to satellites that were directly involved in a system's last merger as *participant satellites*, and the number of participant satellites in a system as its *participation number*.

The post-merger accretion of new, non-participant satellites is not the only factor expected to reduce a system's participation number. For each system, my sample of satellites consists of the 30 most massive satellites at present time. However, participant satellites may be disrupted and fall into the central regions of the merged halo, where they are stripped of mass by dynamical friction. This process may cause even initially massive satellites to be excluded from the observationally motivated sample of the most massive satellites at present time.

To investigate the extent to which satellite participation (or lack theoreof) influences results at present time, the infall times of satellites were determined for all simulated systems. I define the *infall time* of a satellite as the snapshot when it is first recognized as bound to the merger's primary halo. If a satellite falls into the primary halo before being flung out, only to return to its previous bound state in a later snapshot, I define the point of first infall as the satellite's infall time.

Satellites accreted by the secondary halo during a merger are not classified as having fallen in until the secondary halo merges with the primary halo at the end of the

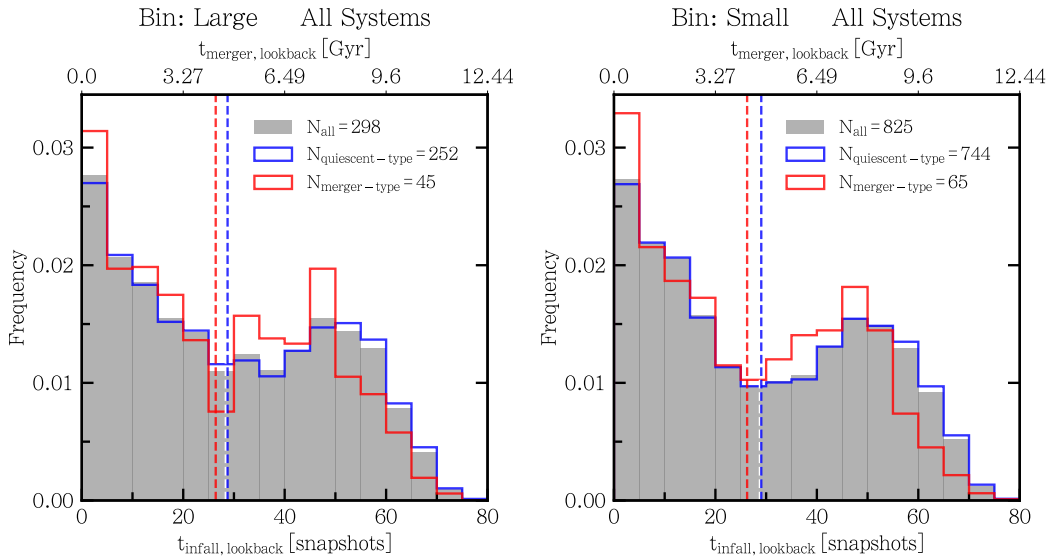

Figure 15: Lookback infall times of all sampled satellites. A compiled list of infall times for all systems, as well as *quiescent-type* and *merger-type* systems specifically, are drawn in shaded gray, blue, and red. Corresponding mean infall times are drawn in white, blue, and red dashed lines respectively.

merger. However, as the primary motivation for the metric of satellite participation is to measure the number of satellites that fell in during or before the merger occurred, it is sufficient for our purposes here.

A distribution of the lookback infall times of sampled satellites is shown in Figure 15. Infall times appear to follow a bimodal distribution for both *quiescent-type* and *merger-type* systems. Distributions for both mass regimes are highly similar.

The number of accreted satellites peak within several snapshots of present time, with a second, smaller peak around 50 snapshots ago, corresponding to a lookback time of around 8 Gyr. For *merger-type* systems, the smaller peak is slightly shifted towards a smaller lookback time, but does not display any significant deviation from the distribution of *quiescent-type* systems.

Even for *merger-type* systems, with at least one major merger within the last 5 Gyr, many sampled satellites have fallen in very recently. This reduces the chance they are affected by the merger. To quantify this, I consider the number of satellites that participated in a system's last major merger for *merger* systems.

Satellite participation can be defined in two ways. On one hand, I define $N_{beforeEnd}$ as the number of satellites – out of the 30 sampled satellites at present time – that fell into either of the merging host haloes before the merger ended. However, this may include satellites from the surrounding environment that were accreted during

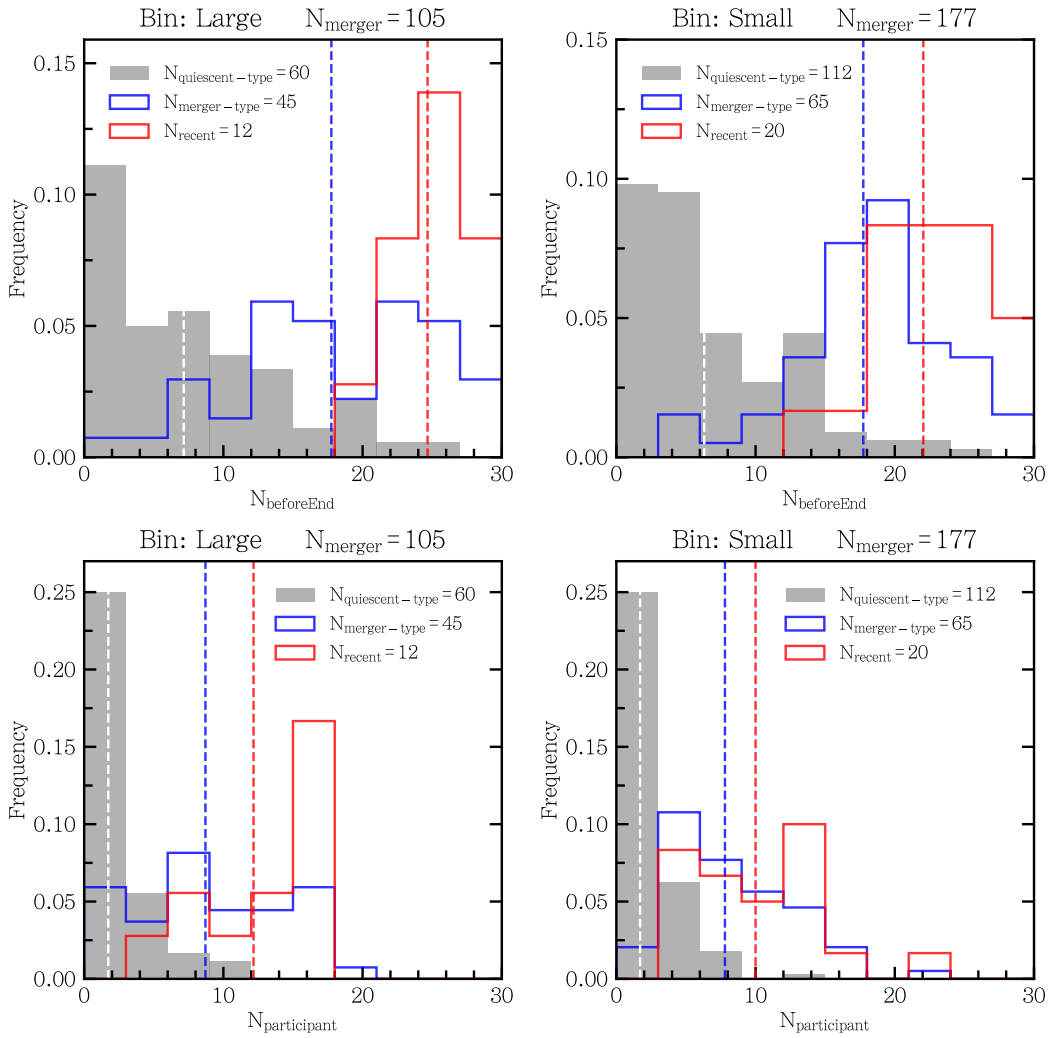

Figure 16: The number of satellites, out of 30 sampled satellites at present time, that participated in the system's last major merger. $N_{beforeEnd}$ represents the number of satellites that fell in before the merger's end, while $N_{participant}$ represents the number of satellites that were accreted before the merger began. Mean values are indicated by white, blue, and red dashed lines for *quiescent-type*, *merger-type*, and *recent* systems respectively. A substantial fraction of the satellite sample selected by mass at present time have not received the full effect from their last merger, washing out the merger's effect.

the merger's duration. Such satellites may not receive a strong influence from the merger's angular momentum.

Thus, I also define $N_{participant}$ as the number of satellites that were bound to either of the two merging haloes before the merger began. Using this metric, we guarantee that each included satellite has experienced the full duration of the merger. I argue that the true number of satellites strongly influenced by a merger lies between

the two populations. $N_{participant}$ and $N_{beforeEnd}$ serve as lower and upper bounds, respectively.

The distribution of satellite participations $N_{participant}$ and $N_{beforeEnd}$ for *merger* systems are shown in Figure 16. For *quiescent-type* systems, up to 20 satellites were accreted before their last merger's end, with at least 10 satellites falling in afterwards. These post-merger accretions do not include satellites temporarily flung out during the merger's duration in my sampling, and a majority of them would have fallen in from the surrounding environment without being strongly affected by the merger. It may be difficult to search for the impact of major mergers before 5 Gyr if selecting satellites by their mass at present time, as most of the merger's influence would be washed out by a substantial number of new satellites.

On the other extreme, most of the satellite population in *recent* systems are accreted before their merger ends, with a mean participation of $N_{beforeEnd} = 25$ satellites. This high participation is more prominent for large-bin systems. Small-bin *recent* systems appear to experience a higher rate of satellite infall, with an average participation of 22 satellites.

The number of sampled satellites involved in a system's merger is substantially lower when considering $N_{participant}$ as a metric instead. For an average *quiescent-type* system, only a small number of satellites $(0 - 6)$ are bound to either of the participating haloes at their merger's beginning. When only considering *merger* systems with a major merger within 5 Gyr of present time, a participation of up to 20 satellites is possible. Interestingly, this maximum is not any higher for *recent* systems, which contain an average of $10 - 12$ participant satellites.

The average of metrics $N_{participant}$ and $N_{beforeEnd}$ can be regarded as an approximate measure of satellite participation. Using this approach, mean participant populations are $4 - 5$ for *quiescent-type* systems, 13 for *merger-type* systems, and $15 - 16$ for *recent* systems. Even for systems with a major merger within the last 2 Gyr, only around $\frac{1}{2}$ of satellites are potentially strongly influenced by the merger, and $\frac{1}{3}$ of the system's satellite population fell in after the merger.

To further illustrate this, $N_{beforeEnd}$ and $N_{participant}$ is plotted for each system against the lookback time to the end of its last major merger (see Figure 17). As expected, a larger lookback time is correlated with a smaller $N_{beforeEnd}$ participant population (Pearson; $r = -0.793$ and $r = -0.835$ for large-bin and small-bin systems).

To reliably measure the extent to which mergers influence satellite distributions, systems with high $N_{beforeEnd}$ and $N_{participant}$ are required. In Figure 17, a lookback

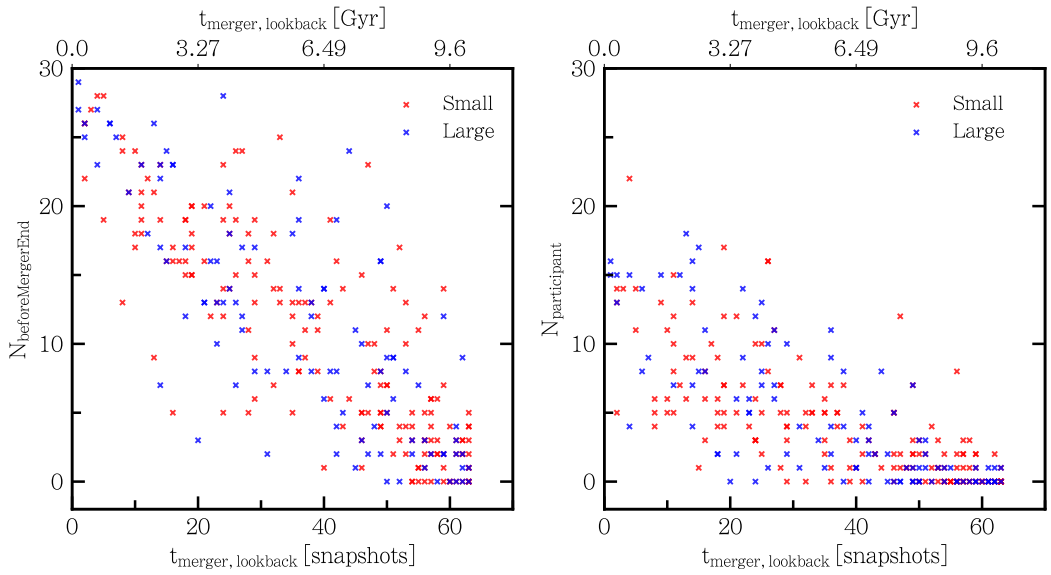

Figure 17: The number of satellites that were accreted before their system's merger began $N_{beforeEnd}$ and the number accreted before their system's merger ended $N_{beforeEnd}$, plotted as a function of lookback time to their merger's end. Earlier mergers result in a lower number of participant satellites in the present-time satellite sample.

time of 10 snapshots (≈ 1.5 Gyr) is required to ensure $N_{beforeEnd} > 20$, which dramatically reduces the number of viable systems. Furthermore, no range of lookback time can consistently achieve $N_{participant} > 15$, which only occurs for some extreme systems.

In summary, mergers may only weakly influence any correlation in present-time satellite galaxy systems due to a substantial fraction of their satellite population being partially or fully uninvolved in their last merger event. This is expected to wash out a large portion of a merger's influence, and may explain the inconclusive results in Section 3. If the model of satellite plane formation put forward by Smith et al. is applicable in a full cosmological context, it would most likely be difficult to observationally confirm despite the planes' proposed long-lived nature due to a washing-out of effects from newly accreted satellites. When only considering the most massive satellites at present time, an approach analogous to observational methods, recent major mergers do not generate strongly correlated satellite planes due to washing-out effects.

4.2 Spatial Distribution of Participant Satellites

In Section 3, I reported that present-time satellite systems with a recent major merger tend to have a similar or slightly weakened degree of phase-space correlation when compared to systems with a quiescent merger history. In Section 4.1, I argued that the influence of mergers is often washed out by the later infall of new satellites and the mass stripping of participant satellites. Until this point, I have focused on an observationally motivated sample of the most massive satellites at present time. However, it is still possible that mergers have a strengthening influence on satellite correlation which is negated by washing-out effects. Thus, I now consider distributions formed strictly of participant satellites at different merger phases.

To do this, the sampling procedure in Section 2.2 was partially repeated, limiting our search to systems known to be *merger* systems. I followed the list of bound subhaloes in order of descending dark matter mass, checking whether they were bound to either of the two participating haloes at the beginning of the system's last merger. Once 30 satellites were found, the list of subhaloes ended, or 1000 subhaloes were checked, I proceeded to the next system.

Correlation parameters such as c/a and Δ_{rms} are affected by the number of satellites in a system. Even an isotropic distribution may appear more flattened if only a small number of satellites are drawn from it. Thus, I only selected systems for which 30 participant satellites were found. 46 large-bin systems and 3 small-bin systems fulfilled this criterion. Due to the dearth of applicable small-bin systems, I limit my investigation to large-bin systems only.

I consider the morphology of participant satellite distributions at three phases of their system's merger. The *start* point, where the participating centrals are at a distance roughly equivalent to the sum of their host haloes' virial radii, is where I define the merger to begin. I define the *after* point as 4 snapshots after the merger's end point, ensuring that the post-merger system stabilizes to some degree. Finally, I consider participant satellite distributions at present time (*now*), along with the corresponding distribution of *observationally motivated* satellites – the latter has already been discussed in previous sections.

In the left-hand panel of Figure 18, the distribution of c/a at the *start*, *after* and *now* points with respect to each system's last major merger is shown. Additionally, we compare plane flattening of participant systems at present time to that of the observationally motivated satellite systems. The difference in c/a between the two

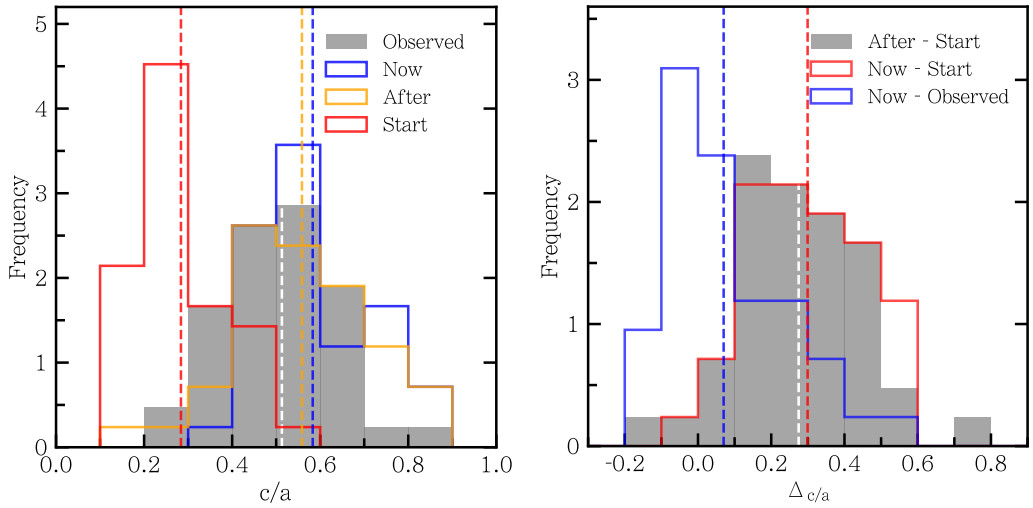

Figure 18: *Left Panel:* c/a of selected large-bin participant satellite systems. c/a at the *start* point, *after* point, and present time are drawn in red, orange, and blue outlines. c/a for corresponding observationally motivated systems, consisting of the most massive satellites at present time, is drawn in shaded gray. Mean values are drawn in red, orange, blue, and white dashed lines respectively. *Right Panel:* c/a shifts between two phases of the system's merger. Shifts are indicated using subtraction of parameters – *e.g.* a decrease in c/a between *start* and *after* points would result in a negative $After - Start$ value.

different samples at present time, along with c/a shifts between different phases in the merger, are also displayed on the right-hand panel.

Participant c/a values increase dramatically between *start* and *after* points over the course of a merger. There is a c/a increase of 0.281, corresponding to a mean shift of 1.7σ with respect to the c/a distribution for *after* point systems. Most of systems experience a c/a gain over this period, with shifts up to 0.6 or more.

This drastic increase in c/a over a merger's duration is an expected result. When tracing participating satellites back in time to the *start* point of the system's last major merger, the satellites are distributed over two separate groups that are about to merge. Naturally, the net distribution's major axis connecting the two groups becomes dominant, resulting in a small c/a value. However, the extent to which this initial group separation is responsible for the c/a increase, rather than effects from the merger itself, is uncertain.

We may loosely estimate the impact of the pre-merger group separation of satellites on c/a as follows. In Section 3.3, I defined a merger to begin when the separation between the two merging centrals is roughly equivalent to the sum of their haloes' virial radii. At this point, the major axis of the participant satellite distribution

should lie along the line connecting the two centrals. Assuming that the post-merger length of the major axis is similar to the merged system's virial radius, the major axis should be roughly twice as long at the merger's beginning. Thus, we may expect c/a to increase by a factor of two between *start* and *after* points. This estimate agrees with the results in Figure 18, which demonstrates a mean c/a increase by a factor of 2.02.

The estimate above assumes that satellites are distributed equally over the two merging groups, implying a near-1:1 mass ratio merger. If group separation is solely responsible, we expect a system's c/a at the start of the merger to be correlated with the merger's mass ratio. For mergers with smaller mass ratios, a majority of participant satellites should belong to the primary halo, rather than being distributed evenly. This should lead to a c/a value that is less skewed by group separation. There is no evidence of any correlation between merger ratio and c/a in *start* point satellite distributions (Pearson; $r = -0.03$, $p = 85\%$).

While the c/a values of participant satellite systems show a dramatic increase during mergers, they appear to stabilize once the mergers end. On average, participant systems experience a 0.2σ shift from the *after* point to present time – a negligible shift.

Next, I compare c/a between participant satellites and observationally motivated satellites at present time. On average, participant systems demonstrate higher c/a by a mean shift of 0.06, corresponding to a 0.5σ significance. However, this shift does not necessarily imply that observationally motivated satellites always form a less-flattened plane than participant satellites. The distribution of the c/a difference between the two samples for each available system, indicated by a blue outline on the right-hand panel of Figure 18, shows that the observationally motivated satellites form a more flattened plane in a non-trivial number of systems. However, observationally motivated satellites can have higher c/a values by up to ≈ 0.2, while participant satellites can do so by up to ≈ 0.6. More often than not, participant satellites – which are all directly influenced by the system's last merger – demonstrate a lower degree of flattening than observationally motivated satellites.

The increase in c/a over the course of a merger appears to depend on its value at the merger's beginning (see Figure 19). There is a strong negative correlation between c/a at a merger's *start* point and $\Delta_{c/a}$ between *start* and *after* points (Pearson; $r = -0.663$, $p = 5 \times 10^{-7}$). This may partially be due to the fact that initially highly flattened distributions as a result of group separation can gain

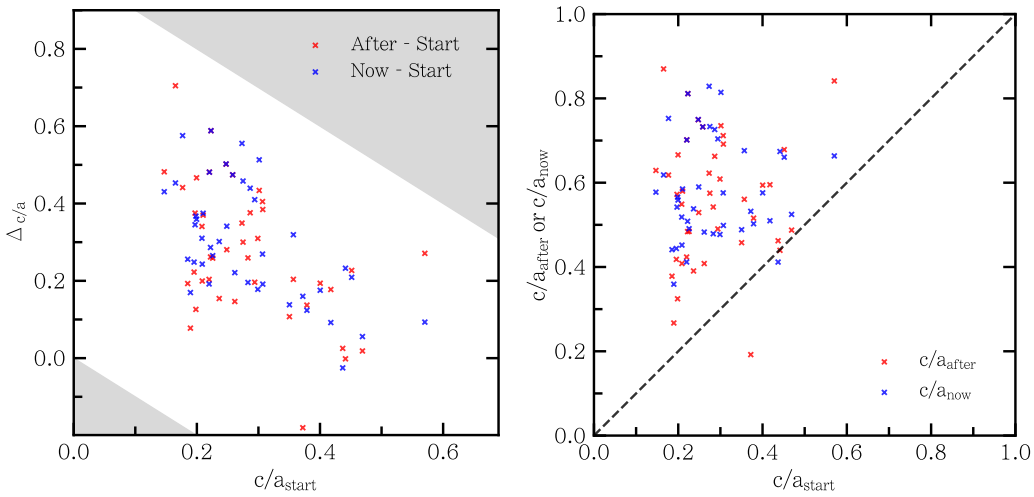

Figure 19: *Left Panel:* Change in c/a of participant satellite systems from their merger's *start* point to their *after* point or present time, against their c/a ratio at their merger's *start* point. This c/a shift is negatively correlated with initial c/a. Grey areas represent regions of c/a changes that are mathematically impossible. *Right Panel:* Comparing participant c/a at different points during their system's merger. The region above the dashed line represents a c/a increase, while the region below represents a c/a decrease. Most systems lose spatial correlation over the course of their merger.

more c/a to reach the range of current values at $0.4 - 0.8$. However, this data may also indicate that mergers have a disrupting effect on the flattening of satellite distributions, preventing the formation of highly flattened systems. Interestingly, this effect is marginally stronger when considering the c/a shift from the *start* point to present time. Disruption from mergers may last longer than expected after they are designated as finished by Sublink.

This result is further illustrated in the right-hand panel of Figure 19. All systems below the black dashed line have experienced a decrease in c/a during the specified period, while systems above the dashed line have experienced an increase in c/a. Only 2 out of 46 systems experienced strengthened flattening until the *after* point, which is reduced to 1 system when considering the total shift until present time. Even systems with initially similar participant c/a can result in a wide variety of c/a values at present time, suggesting a diversity of effects during mergers.

I now consider the impact of mergers on participant satellites when using Δ_{rms} as a metric of flattening instead. In a similar manner as the previous analysis, the distribution of Δ_{rms} across *start*, *after*, and *now* points, as well as the plane height for observationally motivated satellites at present time, is plotted (see left-hand

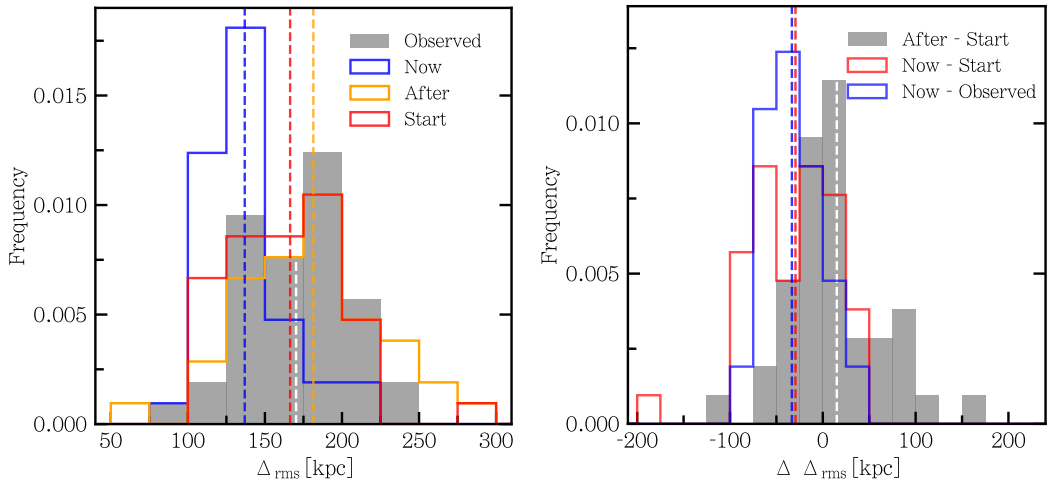

Figure 20: Same as Figure 18, but for Δ_{rms}. On average, participant plane height increases slightly during their merger, but decreases substantially afterwards.

panel, Figure 20). Some systems may experience strong ($\pm$100 kpc) changes in plane height, but there is only a slight mean increase in Δ_{rms} between *start* and *after* points, with a shift of 16 kpc or 0.4σ with respect to the *after* distribution. In the right-hand panel, the distribution of changes in plane height $\Delta\Delta_{rms}$ between *start* and *after* points show that systems can experience increases or decreases in plane height over the course of a merger. This result is consistent with Smith et al., who found that plane height stays unaffected on average by mergers if oriented correctly.

There is a dramatic decrease in Δ_{rms} from the *after* point to present time, with a mean shift of 44 kpc, corresponding to a 1.8σ difference. Even when considering the full period from the merger's *start* point in the right-hand panel of Figure 20, most systems experience a Δ_{rms} decrease. The smaller population of systems that gain Δ_{rms} only do so by up to 50 kpc, while plane height reductions of up to 100 kpc are common. This leads to a similarly drastic disparity in Δ_{rms} between participant and observationally motivated satellites at present time, with a mean difference of 1.0σ.

Interestingly, the mean Δ_{rms} for participant satellites at the beginning of their merger and observationally motivated satellites at present time are highly similar, with only a 5 kpc difference. The distribution of satellites at either point, given that they are yet unaffected by major merger events, have a similar degree of phase-space correlation. The sudden Δ_{rms} decrease may be a result of processes in the aftermath of major mergers.

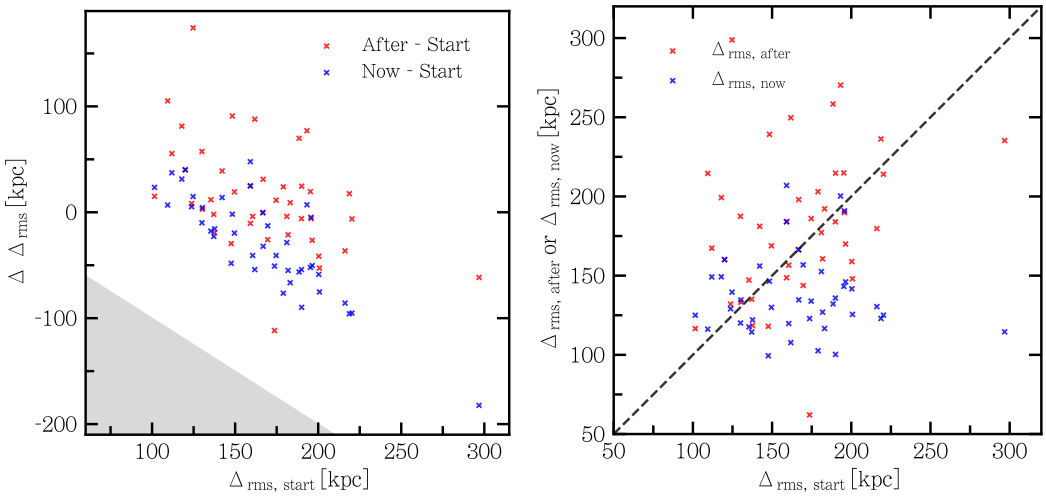

Figure 21: Same as Figure 19, but for Δ_{rms}.

I now check whether the amount of Δ_{rms} gained or lost depends on each system's pre-merger Δ_{rms} value (see Figure 21). Similar to my results for c/a, the change in Δ_{rms} between *start* and *after* points is negatively correlated with the initial plane height of the pre-merger system (Pearson; $r = -0.467$, $p = 0.11\%$). This correlation is stronger still when considering the drastic Δ_{rms} drop after the merger's end as well – there is a correlation of $r = -0.838$ and $p = 10^{-13}$ for the period between the merger's *start* point and present time. Overall, the plane height of present-time participant satellite distributions is strongly linked with the system's pre-merger plane height.

This tendency is further illustrated by the right-hand panel in Figure 21. The number of participant systems with increased or decreased plane heights after their mergers end is similar – there are a comparable number of systems above or below the dashed line that indicates an unchanged Δ_{rms}. However, this scatter is shifted when considering the change in plane height until present time, with more systems losing Δ_{rms}. Interestingly, the initial spread of Δ_{rms} is larger than that at present time (also seen in Figure 20).

Overall, mergers appear to have a two-stage effect on plane heights in my data. During a merger's duration, a system's Δ_{rms} may be increased or decreased, with a slight tendency towards the former. The merger's end is accompanied by a notable drop in plane height until present time. In Figure 20, the participant satellite sample has a lower mean Δ_{rms} by 33 kpc than observationally motivated samples at present time.

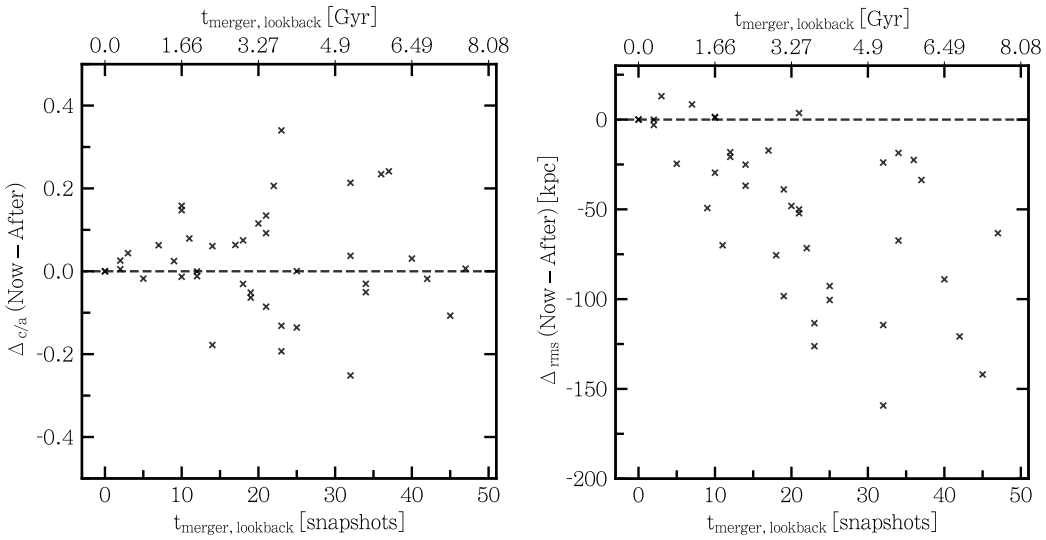

Figure 22: Shifts in c/a and Δ_{rms} from after each system's last merger to present time. c/a is not correlated with the duration of this period, while Δ_{rms} decreases by a larger amount the earlier a system's merger ended.

I suggest that the post-merger Δ_{rms} loss may represent the infall of participant satellites towards the central regions of the merged halo due to dynamical friction, where they are stripped of mass by tidal forces. To illustrate this, the change in c/a and Δ_{rms} between the end of the merger and present time is plotted in Figure 22. The post-merger shift in c/a appears nearly random and uncorrelated with the lookback time to the merger's *after* point (Pearson; $r = 0.039$, $p = 80.0\%$). On the other hand, a vast majority of systems lose Δ_{rms} during this period, with a negative correlation with lookback time (Pearson; $r = -0.559$, $p = 10^{-5}$). Systems that finished their merger early, with a longer duration until present time, appear to experience stronger Δ_{rms} losses. This consistent drop in plane height with time, along with a mostly unaffected c/a ratio, suggests a shrinking of the entire participant satellite distribution's radial extent along with plane height as the satellites fall into the central regions of their host halo.

To verify this, the radial RMS distance d_{rms} of each satellite system to their corresponding central is plotted as a metric of radial extent (see Figure 23). There is a prominent decrease in radial extent throughout the duration of each system's merger, likely due to the separation of the participant satellites in two groups before the merger began. However, I also point out a strong decrease in radial extent after the merger ends, with a mean shift of 121 kpc.

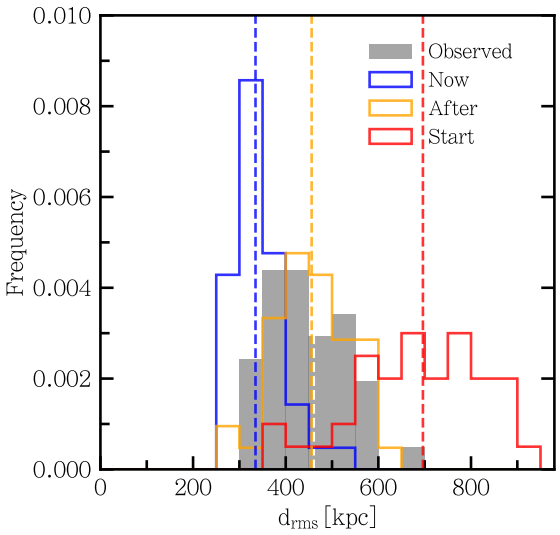

Figure 23: The distribution of participant satellite radial extent d_{rms} at *start*, *after*, and *end* points of a merger, drawn in red, orange, and blue respectively. The radial extent of observationally motivated satellites is shaded in grey. The radial extent of participant satellites is greatly reduced between a merger's *after* point and present time.

Intriguingly, the d_{rms} distribution of observationally motivated satellites at present time is nearly identical to that for participant satellites at their *after* point, with a KS test returning a 79% chance that they are drawn from the same distribution. This supports the hypothesis that post-merger satellites fall in towards the central regions of their host halo, while the accretion of new satellites from the local environment maintains the radial extent of the observationally motivated set of the most massive satellites.

4.3 Impact on Orbital Correlation

I now consider the degree of kinematic correlation $\angle_{rms}$ in different phases of a merger (see upper panels in Figure 24). The mean $\angle_{rms}$ values at *start*, *after*, and *end* points are nearly identical, with a negligible 0.1σ shift between each stage. In the right-hand panel, systems may gain or lose up to 10° over the course of a merger, but with a mean shift of 0°. The $\angle_{rms}$ distribution of participant and observationally motivated satellite systems are also highly similar, with the latter only higher by 1° on average. This suggests that in general, mergers do not significantly change the degree of kinematic correlation in satellite systems. Some extreme participant

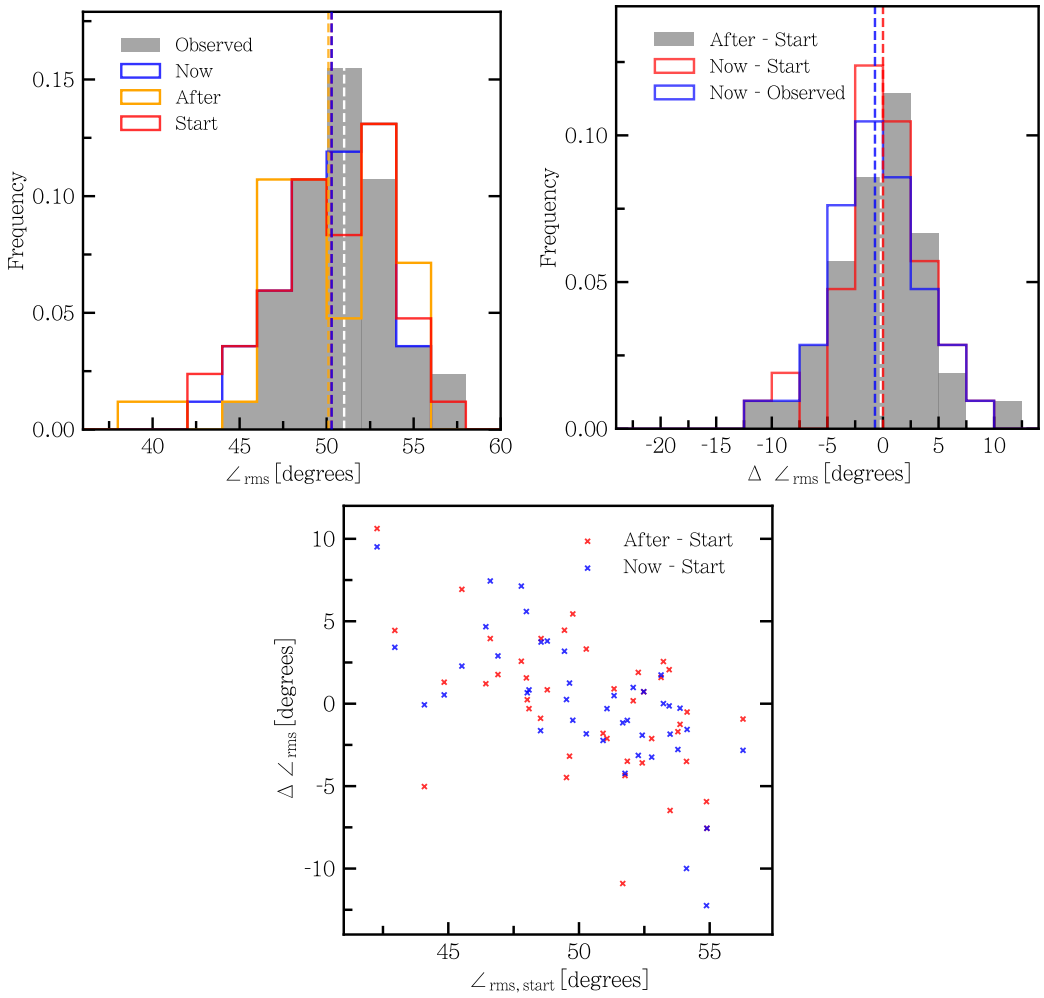

Figure 24: *Upper Panels:* Same as Figure 18, but for $\angle_{rms}$. On the left-hand panel, the red dashed line indicating the mean value at mergers' *start* points is obscured by the orange dashed line indicating the mean value at mergers' *after* points. *Lower Panel:* The change in $\angle_{rms}$ over a given period is negatively correlated with its pre-merger value. Recent mergers do not appear to significantly modify the degree of orbital correlation in participant systems.

systems temporarily achieve $\angle_{rms} \approx 38°$ after their merger ends, but such values are not seen at present time with a minimum of 42°.

In the lower panel in Figure 24, the change in $\angle_{rms}$ until a merger's *after* point or to present time is compared with its pre-merger value. The *start-after* shift and $\angle_{rms}$ at the *start* point are weakly negatively correlated (Pearson; $r = -0.541$, $p = 10^{-4}$). This correlation is stronger when considering the shift until present time (Pearson; $r = -0.700$, $p = 10^{-8}$).

In summary, mergers do not consistently strengthen or weaken the degree of kinematic correlation in participant satellite systems. However, they appear to disrupt more correlated systems, preventing the formation of highly kinematically correlated systems. I do not find any evidence that mergers produce satellite planes with cohesive satellite orbits.

5 Conclusions

In this dissertation, I have investigated the impact of merger events on satellite phase-space distributions in the IllustrisTNG hydrodynamic cosmological simulation. In Section 3.2, I found that mergers appear to have a negligible or slightly negative influence on the systems' degree of spatial and kinematic correlation when considering systems of satellites selected by their mass at present time. Systems with major mergers within the last 2 Gyr demonstrate a thicker plane height and weakened orbital correlation when compared to those with a quiescent merger history. There is no strong link between a merger's mass ratio and its impact on the resultant satellite distribution at present time.

In Section 3.4, I determined that mergers with a larger specific angular momentum content – corresponding to haloes with a more circular initial infall trajectory – is weakly linked to a more stable merger plane. A stable merger plane, in turn, weakly corresponds to a better alignment between the merger plane and the best-fit plane or orbital plane of the merged satellite system. These trends are generally inconclusive, defined by a visual dearth of systems with a specific combination of parameter values than statistically significant correlations. I also report that systems with well-aligned merger planes and best-fit planes at present time tend to have a stronger degree of spatial and kinematic correlation. Mergers may occasionally improve the phase-space correlation in a satellite system if oriented correctly. However, no highly correlated systems are formed in this manner within the limited sample of the considered simulation.

In Section 4.1, I discussed the role of late-infall satellites in washing out any signal from earlier mergers. I found that systems with major mergers within the last 5 Gyr tend to have accreted more than one half of their satellite population before their last merger's completion. However, satellites that were bound to their current halo before its last major merger began are rare. Even systems with mergers within the last 2 Gyr are not generally populated with more than 50% of such satellites. I argue that this is the primary cause of the weakened influence mergers have on observationally motivated satellite systems, which consist of the most massive satellites at present time.

When only considering satellites which participated in the entirety of their system's merger in Section 4.2 and Section 4.3, I find a more cohesive result. Mergers appear to have a disrupting effect on initially correlated systems – satellite distributions that are flattened or orbitally correlated before their merger begins lose their co-

hesion throughout their merger's duration. Most pre-merger systems demonstrate a strongly flattened satellite distribution, which is thought to be a result of their satellites being distributed over two merging groups. However, while the ratio of satellites in either group should depend on their merger's mass ratio, I find no correlation between a system's pre-merger flattening and its merger mass ratio. Additionally, there is a consistent post-merger reduction in plane heights and radial extents of satellite systems until present time.

Based on the results above, I suggest the following. During a merger event, the spatial and kinematic correlation within the participating satellite distribution is disrupted, preventing the formation or continued existence of highly flattened or orbitally correlated systems. During the merger, the radial extent of the satellite distribution shrinks as accreted satellites are slowed by dynamical friction and enter a radial infall trajectory. Systems that are well-aligned with the merger's plane of interaction, which are slightly more common for stable mergers with a high angular momentum content, may experience a slight improvement in phase-space correlation. However, this effect is generally washed out by disruption from the merger itself.

After the merger is complete, participating satellites continue to fall in towards the central regions of their host halo, losing mass to stripping in the process. When this mass stripping occurs, the participating satellites cease to be among the highest-mass satellites in the system, making any theoretical attempts at observation difficult. When considering a observationally motivated sample of satellites ranked by their mass at present time, a substantial fraction of the sampled satellite population would have been accreted post-merger, washing out the effects from their system's last major merger.

Mergers do not typically generate long-lived, highly correlated satellite planes in a full cosmological context as realized by IllustrisTNG. While I fail to confirm a plane-forming mechanism as proposed by Smith et al., this may be due to the low initial satellite radial extents used in their N-body simulations. While Smith et al. begin with a satellite spread of 40 kpc along their merger's axis of interaction, most of the pre-merger systems with Centaurus A-like halo masses demonstrate distribution minor axes of $100 - 220$ kpc. In Smith et al., the angular momentum injected into a satellite system by a merger slings satellites outwards while maintaining the distribution's height, resulting in flattened planes. In a full cosmological context, the high pre-merger distribution minor axes may prevent the slinging of satellites from occurring. Instead, mergers result in the disruption of phase-space correlation in satellite systems and a reduction of participating satellites' radial extent.

While mergers may disrupt and prevent the formation of highly correlated satellite systems in most cases, they can also strengthen a system's degree of phase-space correlation in rare cases. If a system experienced a major merger recently (within 2 Gyr), the comparatively low number of satellites accreted post-merger may allow the observation of this positive effect. The properties of the Centaurus A system are consistent with a major merger within 2 Gyr, with a mass ratio of up to 1.5 (Wang et al.). The intriguing satellite structure around Centaurus A may be partially explained by Smith et al.'s model of satellite plane formation, wherein satellites are flung outwards during a well-oriented merger while the distribution of satellites orthogonal to the merger plane remains mostly constant.

In future work, it may be worthwhile to explore the Centaurus A merger in detail, and whether the system's satellite distribution is compatible with a potential merger origin. One approach would be to model the orbits of Centaurus A's satellite galaxies using their new line-of-sight velocities obtained by Müller et al. while assuming a range of possible tangential velocities, and identifying satellites that have fallen in recently. By finding a sample of satellites that participated in the Centaurus A merger, the washing-out effect from recent accretions can be mitigated. On the other hand, we may identify Centaurus A analogs in dark matter-only constrained simulations, which feature a substantially higher resolution than IllustrisTNG. By modelling the kinematics of past mergers of simulated systems in detail, it may be possible to identify individual cases where a merger event reproduces the flattening and co-rotation observed for the CASP.

In general, however, this study has demonstrated that most merger events do not facilitate the formation of highly flattened or kinematically correlated planes of (dark matter-dominated) satellite galaxies. If such anisotropic structures prove to be ubiquitous outside of the Local Volume, and not a coincidental result of the unique history of Local Volume host galaxies, mergers will be fully ruled out as a dominant formation mechanism – it is doubtful that all systems hosting satellite planes have had a non-quiescent merger history. The Planes of Satellite Galaxies Problem does not appear to be alleviated by recent major mergers, and remains an unsolved problem for the ΛCDM model of cosmology.

References

Abbott, T. M. C., F. B. Abdalla, S. Allam, A. Amara, J. Annis, J. Asorey, S. Avila, et al. "The Dark Energy Survey: Data Release 1". *The Astrophysical Journal Supplement Series* 239 (2018): 18. https://doi.org/10.3847/1538-4365/aae9f0.

Bılek, M., I. Thies, P. Kroupa, and B. Famaey. "MOND simulation suggests an origin for some peculiarities in the Local Group". *Astronomy and Astrophysics* 614 (2018): A59. https://doi.org/10.1051/0004-6361/201731939.

Blanton, M. R., M. A. Bershady, B. Abolfathi, F. D. Albareti, C. Allende Prieto, A. Almeida, J. Alonso-Garcıa, et al. "Sloan Digital Sky Survey IV: Mapping the Milky Way, Nearby Galaxies, and the Distant Universe". *The Astronomical Journal* 154 (2017): 28. https://doi.org/10.3847/1538-3881/aa7567.

Boylan-Kolchin, M., V. Springel, S. D. White, A. Jenkins, and G. Lemson. "Resolving cosmic structure formation with the Millennium-II Simulation". *Monthly Notices of the Royal Astronomical Society* 398 (2009): 1150–1164. https://doi.org/10.1111/j.1365-2966.2009.15191.x.

Brainerd, T. G. "Anisotropic Distribution of SDSS Satellite Galaxies: Planar (Not Polar) Alignment". *The Astrophysical Journal* 628 (2005): L101–L104. https://doi.org/10.1086/432713.

Chiboucas, K., B. A. Jacobs, R. B. Tully, and I. D. Karachentsev. "Confirmation of faint dwarf galaxies in the M81 group". *The Astronomical Journal* 146 (2013): 126. https://doi.org/10.1088/0004-6256/146/5/126.

Collins, M. L., N. F. Martin, R. M. Rich, R. A. Ibata, S. C. Chapman, A. W. McConnachie, A. M. Ferguson, M. J. Irwin, and G. F. Lewis. "Comparing the observable properties of dwarf galaxies on and off the andromeda plane". *Astrophysical Journal Letters* 799 (2015): 13. https://doi.org/10.1088/2041-8205/799/1/L13.

Conn, A. R., G. F. Lewis, R. A. Ibata, Q. A. Parker, D. B. Zucker, A. W. McConnachie, N. F. Martin, et al. "The three-dimensional structure of the m31 satellite system; Strong evidence for an inhomogeneous distribution of satellites". *The Astrophysical Journal* 766 (2013): 120. https://doi.org/10.1088/0004-637X/766/2/120.

Crnojević, D., E. K. Grebel, and A. Koch. "A close look at the Centaurus A group of galaxies. I. Metallicity distribution functions and population gradients in early-type dwarfs". *Astronomy and Astrophysics* 516 (2010): A85. https://doi.org/10.1051/0004-6361/200913429.

D'Souza, R., and E. F. Bell. "The Andromeda galaxy's most important merger about 2 billion years ago as M32's likely progenitor". *Nature Astronomy* 2 (2018): 737–743. https://doi.org/10.1038/s41550-018-0533-x.

Davis, M., G. Efstathiou, C. S. Frenk, and S. D. M. White. "The evolution of large-scale structure in a universe dominated by cold dark matter". *The Astrophysical Journal* 292 (1985): 371. https://doi.org/10.1086/163168.

Eckert, D., M. Jauzac, H. Shan, J.-P. Kneib, T. Erben, H. Israel, E. Jullo, et al. "Warm-hot baryons comprise 5-10 per cent of filaments in the cosmic web". *Nature* 528 (2015): 105–107. https://doi.org/10.1038/nature16058.

Fattahi, A., J. F. Navarro, T. Sawala, C. S. Frenk, L. V. Sales, K. Oman, M. Schaller, and J. Wang. "The cold dark matter content of Galactic dwarf spheroidals: no cores, no failures, no problem". *arXiv e-prints* (2016). arXiv: 1607.06479.

Fouquet, S., F. Hammer, Y. Yang, M. Puech, and H. Flores. "Does the dwarf galaxy system of the Milky Way originate from Andromeda?" *Monthly Notices of the Royal Astronomical Society* 427 (2012): 1769–1783. https://doi.org/10.1111/j.1365-2966.2012.22067.x.

Garrison-Kimmel, S., A. Wetzel, J. S. Bullock, P. F. Hopkins, M. Boylan-Kolchin, C. A. Faucher-Giguère, D. Kereš, et al. "Not so lumpy after all: Modelling the depletion of dark matter subhaloes by Milky Way-like galaxies". *Monthly Notices of the Royal Astronomical Society* 471 (2017): 1709–1727. https://doi.org/10.1093/MNRAS/STX1710.

Geha, M., R. H. Wechsler, Y.-Y. Mao, E. J. Tollerud, B. Weiner, R. Bernstein, B. Hoyle, et al. "The SAGA Survey. I. Satellite Galaxy Populations around Eight Milky Way Analogs". *The Astrophysical Journal* 847 (2017): 4. https://doi.org/10.3847/1538-4357/aa8626.

Grebel, E. K., T. Kolatt, and W. Brandner. "Orbits versus Star Formation Histories: A Progress Report". Ed. by P. Whitelock and R. Cannon. *The Stellar Content of Local Group Galaxies*, IAU Symposium, 192 (1999): 447.

Hammer, F., Y. B. Yang, J. L. Wang, R. Ibata, H. Flores, and M. Puech. "A 2-3 billion year old major merger paradigm for the Andromeda galaxy and its outskirts". *Monthly Notices of the Royal Astronomical Society* 475 (2018): 2754–2767. https://doi.org/10.1093/mnras/stx3343.

Hammer, F., Y. Yang, S. Fouquet, M. S. Pawlowski, P. Kroupa, M. Puech, H. Flores, and J. Wang. "The vast thin plane of M31 corotating dwarfs: An additional fossil signature of the M31 merger and of its considerable impact in the whole local group". *Monthly Notices of the Royal Astronomical Society* 431 (2013): 3543–3549. https://doi.org/10.1093/mnras/stt435.

Haslbauer, M., J. Dabringhausen, P. Kroupa, B. Javanmardi, and I. Banik. "Galaxies lacking dark matter in the Illustris simulation". *Astronomy and Astrophysics* 626 (2019): A47. https://doi.org/10.1051/0004-6361/201833771.

Hubble, E. P. "A spiral nebula as a stellar system, Messier 31." *The Astrophysical Journal* 69 (1929): 103–158. https://doi.org/10.1086/143167.

Ibata, N., R. Ibata, B. Famaey, and G. F. Lewis. "Velocity anti-correlation of diametrically opposed galaxy satellites in the low-redshift Universe". *Nature* 511 (2014): 563–566. https://doi.org/10.1038/nature13481.

Ibata, R. A., N. G. Ibata, G. F. Lewis, N. F. Martin, A. Conn, P. Elahi, V. Arias, and N. Fernando. "A thousand shadows of andromeda: Rotating planes of satellites in the millennium-II cosmological simulation". *Astrophysical Journal Letters* 784 (2014): 6. https://doi.org/10.1088/2041-8205/784/1/L6.

Ibata, R. A., G. F. Lewis, A. R. Conn, M. J. Irwin, A. W. McConnachie, S. C. Chapman, M. L. Collins, et al. "A vast, thin plane of corotating dwarf galaxies orbiting the Andromeda galaxy". *Nature* 493 (2013): 62–65. https://doi.org/10.1038/nature11717.

Karachentsev, I. D., V. E. Karachentseva, W. K. Huchtmeier, and D. I. Makarov. "A Catalog of Neighboring Galaxies". *The Astronomical Journal* 127 (2004): 2031–2068. https://doi.org/10.1086/382905.

Kirby, E. N., J. G. Cohen, P. Guhathakurta, L. Cheng, J. S. Bullock, and A. Gallazzi. "The Universal Stellar Mass-Stellar Metallicity Relation for Dwarf Galaxies". *The Astrophysical Journal* 779 (2013): 102. https://doi.org/10.1088/0004-637X/779/2/102.

Koposov, S. E., V. Belokurov, G. Torrealba, and N. W. Evans. "Beasts of the Southern Wild: Discovery of Nine Ultra Faint Satellites in the Vicinity of the Magellanic Clouds." *The Astrophysical Journal* 805 (2015): 130. https://doi.org/10.1088/0004-637X/805/2/130.

Kravtsov, A. V., A. A. Klypin, and A. M. Khokhlov. "Adaptive Refinement Tree: A New High-Resolution N-Body Code for Cosmological Simulations". *The Astrophysical Journal Supplement Series* 111 (1997): 73–94. https://doi.org/10.1086/313015.

Kroupa, P. "The dark matter crisis: Falsification of the current standard model of cosmology". *Publications of the Astronomical Society of Australia* 29 (2012): 395–433. https://doi.org/10.1071/AS12005.

Kroupa, P., C. Theis, and C. M. Boily. "The great disk of Milky-Way satellites and cosmological sub-structures". *Astronomy and Astrophysics* 431 (2005): 517–521. https://doi.org/10.1051/0004-6361:20041122.

Kunkel, W. E., and S. Demers. "The Magellanic Plane". 182 (1976): 241.

Li, Y. S., and A. Helmi. "Infall of substructures on to a Milky Way-like dark halo". *Monthly Notices of the Royal Astronomical Society* 385 (2008): 1365–1373. https://doi.org/10.1111/j.1365-2966.2008.12854.x.

Libeskind, N. I., C. S. Frenk, S. Cole, J. C. Helly, A. Jenkins, J. F. Navarro, and C. Power. "The distribution of satellite galaxies: The great pancake". *Monthly Notices of the Royal Astronomical Society* 363 (2005): 146–152. https://doi.org/10.1111/j.1365-2966.2005.09425.x.

Libeskind, N. I., A. Knebe, Y. Hoffman, S. Gottlöber, G. Yepes, and M. Steinmetz. "The preferred direction of infalling satellite galaxies in the Local Group". *Monthly Notices of the Royal Astronomical Society* 411 (2011): 1525–1535. https://doi.org/10.1111/j.1365-2966.2010.17786.x.

Lovell, M. R., V. R. Eke, C. S. Frenk, and A. Jenkins. "The link between galactic satellite orbits and subhalo accretion". *Monthly Notices of the Royal Astronomical Society* 413 (2011): 3013–3021. https://doi.org/10.1111/j.1365-2966.2011.18377.x.

Lynden-Bell, D. "Dwarf Galaxies and Globular Clusters in High Velocity Hydrogen Streams". *Monthly Notices of the Royal Astronomical Society* 174 (1976): 695–710. https://doi.org/10.1093/mnras/174.3.695.

McAlpine, S., J. C. Helly, M. Schaller, J. W. Trayford, Y. Qu, M. Furlong, R. G. Bower, et al. "The EAGLE simulations of galaxy formation: Public release of halo and galaxy catalogues". *Astronomy and Computing* 15 (2016): 72–89. https://doi.org/10.1016/j.ascom.2016.02.004.

McConnachie, A. W., M. J. Irwin, R. A. Ibata, J. Dubinski, L. M. Widrow, N. F. Martin, P. Côté, et al. "The remnants of galaxy formation from a panoramic survey of the region around M31". *Nature* 461 (2009): 66–69. https://doi.org/10.1038/nature08327.

Metz, M., and P. Kroupa. "Dwarf spheroidal satellites: Are they of tidal origin?" *Monthly Notices of the Royal Astronomical Society* 376 (2007): 387–392. https://doi.org/10.1111/j.1365-2966.2007.11438.x.

Metz, M., P. Kroupa, and H. Jerjen. "Discs of satellites: The new dwarf spheroidals". *Monthly Notices of the Royal Astronomical Society* 394 (2009): 2223–2228. https://doi.org/10.1111/j.1365-2966.2009.14489.x.

Metz, M., P. Kroupa, C. Theis, G. Hensler, and H. Jerjen. "Did the milky way dwarf satellites enter the halo as a group?" *The Astrophysical Journal* 697 (2009): 269–274. https://doi.org/10.1088/0004-637X/697/1/269.

Milgrom, M. "A modification of the Newtonian dynamics as a possible alternative to the hidden mass hypothesis". *The Astrophysical Journal* 270 (1983): 365. https://doi.org/10.1086/161130.

Moore, B., S. Ghigna, F. Governato, G. Lake, T. Quinn, J. Stadel, and P. Tozzi. "Dark Matter Substructure within Galactic Halos". *The Astrophysical Journal* 524 (1999): L19–L22. https://doi.org/10.1086/312287.

Müller, O., M. S. Pawlowski, H. Jerjen, and F. Lelli. "A whirling plane of satellite galaxies around Centaurus A challenges cold dark matter cosmology". *Science* 359 (2018): 534–537. https://doi.org/10.1126/science.aao1858.

Müller, O., M. S. Pawlowski, F. Lelli, K. Fahrion, M. Rejkuba, M. Hilker, J. Kanehisa, N. Libeskind, and H. Jerjen. "The coherent motion of Cen A dwarf satellite galaxies remains a challenge for ΛCDM cosmology". *arXiv e-prints* (2020). arXiv: 2012.08138.

Müller, O., M. Rejkuba, M. S. Pawlowski, R. Ibata, F. Lelli, M. Hilker, and H. Jerjen. "The dwarf galaxy satellite system of Centaurus A". *Astronomy and Astrophysics* 629 (2019): A18. https://doi.org/10.1051/0004-6361/201935807.

Müller, O., R. Scalera, B. Binggeli, and H. Jerjen. "The M 101 group complex: New dwarf galaxy candidates and spatial structure". *Astronomy and Astrophysics* 602 (2017). https://doi.org/10.1051/0004-6361/201730434.

Nadler, E. O., R. H. Wechsler, K. Bechtol, Y. .-. Mao, G. Green, A. Drlica-Wagner, M. McNanna, et al. "Milky Way Satellite Census. II. Galaxy-Halo Connection Constraints Including the Impact of the Large Magellanic Cloud". *The Astrophysical Journal* 893 (2020): 48. https://doi.org/10.3847/1538-4357/ab846a.

Okazaki, T., and Y. Taniguchi. "Dwarf Galaxy Formation Induced by Galaxy Interactions". *The Astrophysical Journal* 543 (2000): 149–152. https://doi.org/10.1086/317109.

Pawlowski, M. S., P. Kroupa, G. Angus, K. S. de Boer, B. Famaey, and G. Hensler. "Filamentary accretion cannot explain the orbital poles of the Milky Way satellites". *Monthly Notices of the Royal Astronomical Society* 424 (2012): 80–92. https://doi.org/10.1111/j.1365-2966.2012.21169.x.

Pawlowski, M. S., P. Kroupa, and K. S. De Boer. "Making counter-orbiting tidal debris: The origin of the Milky Way disc of satellites?" *Astronomy and Astrophysics* 532 (2011): A118. https://doi.org/10.1051/0004-6361/201015021.

Pawlowski, M. S., J. Pflamm-Altenburg, and P. Kroupa. "The VPOS: A vast polar structure of satellite galaxies, globular clusters and streams around the Milky Way". *Monthly Notices of the Royal Astronomical Society* 423 (2012): 1109–1126. https://doi.org/10.1111/j.1365-2966.2012.20937.x.

Pawlowski, M. S. "The planes of satellite galaxies problem, suggested solutions, and open questions". *Modern Physics Letters A* 33 (2018): 1830004. https://doi.org/10.1142/S0217732318300045.

Pawlowski, M. S., J. S. Bullock, T. Kelley, and B. Famaey. "Do Halos that Form Early, Have High Concentration, Are Part of a Pair, or Contain a Central Galaxy Potential Host More Pronounced Planes of Satellite Galaxies?" *The Astrophysical Journal* 875 (2019): 105. https://doi.org/10.3847/1538-4357/ab10e0.

Pawlowski, M. S., B. Famaey, H. Jerjen, D. Merritt, P. Kroupa, J. Dabringhausen, F. Lüghausen, et al. "Co-orbiting satellite galaxy structures are still in conflict with the distribution of primordial dwarf galaxies". *Monthly Notices of the Royal Astronomical Society* 442 (2014): 2362–2380. https://doi.org/10.1093/mnras/stu1005.

Pawlowski, M. S., B. Famaey, D. Merritt, and P. Kroupa. "On the persistence of two small-scale problems in ΛCDM". *The Astrophysical Journal* 815 (2015): 19. https://doi.org/10.1088/0004-637X/815/1/19.

Pawlowski, M. S., and P. Kroupa. "The Milky Way's disc of classical satellite galaxies in light of Gaia DR2". *Monthly Notices of the Royal Astronomical Society* 491 (2020): 3042–3059. https://doi.org/10.1093/mnras/stz3163.

Pawlowski, M. S., S. S. McGaugh, and H. Jerjen. "The new Milky Way satellites: Alignment with the VPOS and predictions for proper motions and velocity dispersions". *Monthly Notices of the Royal Astronomical Society* 453 (2015): 1047–1061. https://doi.org/10.1093/mnras/stv1588.

Pillepich, A., D. Nelson, L. Hernquist, V. Springel, R. Pakmor, P. Torrey, R. Weinberger, et al. "First results from the IllustrisTNG simulations: the stellar mass content of groups and clusters of galaxies". *Monthly Notices of the Royal Astronomical Society* 475 (2018): 648–675. https://doi.org/10.1093/mnras/stx3112.

Planck Collaboration. "Planck 2015 results: XIII. Cosmological parameters". *Astronomy and Astrophysics* 594 (2016): A13. https://doi.org/10.1051/0004-6361/201525830.

Ploeckinger, S., S. Recchi, G. Hensler, and P. Kroupa. "Chemodynamical evolution of tidal dwarf galaxies - II. The long-term evolution and influence of a tidal field". *Monthly Notices of the Royal Astronomical Society* 447 (2015): 2512–2525. https://doi.org/10.1093/mnras/stu2629.

Ploeckinger, S., K. Sharma, J. Schaye, R. A. Crain, M. Schaller, and C. Barber. "Tidal dwarf galaxies in cosmological simulations". *Monthly Notices of the Royal Astronomical Society* 474 (2018): 580–596. https://doi.org/10.1093/mnras/stx2787.

Rodriguez-Gomez, V., S. Genel, M. Vogelsberger, D. Sijacki, A. Pillepich, L. V. Sales, P. Torrey, et al. "The merger rate of galaxies in the Illustris simulation: a comparison with observations and semi-empirical models". *Monthly Notices of the Royal Astronomical Society* 449 (2015): 49–64. https://doi.org/10.1093/mnras/stv264.

Shao, S., M. Cautun, C. S. Frenk, R. J. Grand, F. A. Gómez, F. Marinacci, and C. M. Simpson. "The multiplicity and anisotropy of galactic satellite accretion". *Monthly Notices of the Royal Astronomical Society* 476 (2018): 1796–1810. https://doi.org/10.1093/mnras/sty343.

Shapley, H. "Remarks on the Arrangement of the Sidereal Universe". *The Astrophysical Journal* 49 (1919): 311–336.

Smith, R., P. A. Duc, F. Bournaud, and S. K. Yi. "a Formation Scenario for the Disk of Satellites: Accretion of Satellites During Mergers". *The Astrophysical Journal* 818 (2016): 11. https://doi.org/10.3847/0004-637x/818/1/11.

Springel, V., R. Pakmor, A. Pillepich, R. Weinberger, D. Nelson, L. Hernquist, M. Vogelsberger, et al. "First results from the IllustrisTNG simulations: matter and galaxy clustering". *Monthly Notices of the Royal Astronomical Society* 475 (2018): 676–698. https://doi.org/10.1093/mnras/stx3304.

Springel, V., J. Wang, M. Vogelsberger, A. Ludlow, A. Jenkins, A. Helmi, J. F. Navarro, C. S. Frenk, and S. D. M. White. "The Aquarius Project: the subhalos of galactic halos". *Monthly Notices of the Royal Astronomical Society* 391 (2008): 1685–1711. https://doi.org/10.1111/j.1365-2966.2008.14066.x.

Springel, V., N. Yoshida, and S. D. M. White. "GADGET: a code for collisionless and gasdynamical cosmological simulations". *New Astronomy* 6 (2001): 79–117. https://doi.org/10.1016/S1384-1076(01)00042-2.

Tamm, A., E. Tempel, P. Tenjes, O. Tihhonova, and T. Tuvikene. "Stellar mass map and dark matter distribution in M 31". *Astronomy and Astrophysics* 546 (2012): A4. https://doi.org/10.1051/0004-6361/201220065.

Taylor, C., M. Boylan-Kolchin, P. Torrey, M. Vogelsberger, and L. Hernquist. "The mass profile of the Milky Way to the virial radius from the Illustris simulation". *Monthly Notices of the Royal Astronomical Society* 461 (2016): 3483–3493. https://doi.org/10.1093/mnras/stw1522.

Tully, R. B. "Galaxy groups 54". *The Astronomical Journal* 149 (2015): 54. https://doi.org/10.1088/0004-6256/149/2/54.

Vera-Ciro, C. A., L. V. Sales, A. Helmi, C. S. Frenk, J. F. Navarro, V. Springel, M. Vogelsberger, and S. D. White. "The shape of dark matter haloes the Aquarius simulations: Evolution and memory". *Monthly Notices of the Royal Astronomical Society* 416 (2011): 1377–1391. https://doi.org/10.1111/j.1365-2966.2011.19134.x.

Virtanen, P., R. Gommers, T. E. Oliphant, M. Haberland, T. Reddy, D. Cournapeau, E. Burovski, et al. "SciPy 1.0: Fundamental Algorithms for Scientific Computing in Python". *Nature Methods* 17 (2020): 261–272. https://doi.org/10.1038/s41592-019-0686-2.

Vogelsberger, M., S. Genel, V. Springel, P. Torrey, D. Sijacki, D. Xu, G. Snyder, D. Nelson, and L. Hernquist. "Introducing the Illustris Project: simulating the coevolution of dark and visible matter in the Universe". *Monthly Notices of the Royal Astronomical Society* 444 (2014): 1518–1547. https://doi.org/10.1093/mnras/stu1536.

Wang, J., F. Hammer, M. Rejkuba, D. Crnojević, and Y. Yang. "A recent major merger tale for the closest giant elliptical galaxy Centaurus A". *Monthly Notices of the Royal Astronomical Society* 498 (2020): 2766–2777. https://doi.org/10.1093/mnras/staa2508.

Wang, J., C. S. Frenk, and A. P. Cooper. "The spatial distribution of galactic satellites in the Λ cold dark matter cosmology". *Monthly Notices of the Royal Astronomical Society* 429 (2013): 1502–1513. https://doi.org/10.1093/mnras/sts442.

Wolf, J., G. D. Martinez, J. S. Bullock, M. Kaplinghat, M. Geha, R. R. Muñoz, J. D. Simon, and F. F. Avedo. "Accurate masses for dispersion-supported galaxies". *Monthly Notices of the Royal Astronomical Society* 406 (2010): 1220–1237. https://doi.org/10.1111/j.1365-2966.2010.16753.x.

Yang, X., F. C. Van Den Bosch, H. J. Mo, S. Mao, X. Kang, S. M. Weinmann, Y. Guo, and Y. P. Jing. "The alignment between the distribution of satellites and the orientation of their central galaxy". *Monthly Notices of the Royal Astronomical Society* 369 (2006): 1293–1302. https://doi.org/10.1111/j.1365-2966.2006.10373.x.

Zentner, A. R., A. V. Kravtsov, O. Y. Gnedin, and A. A. Klypin. "The Anisotropic Distribution of Galactic Satellites". *The Astrophysical Journal* 629 (2005): 219–232. https://doi.org/10.1086/431355.